

The maximally entangled symmetric state in terms of the geometric measure

Martin Aulbach,^{1,2,3,*} Damian Markham,^{4,1,†} and Mio Murao^{1,5,‡}

¹*Department of Physics, Graduate School of Science,
The University of Tokyo, Tokyo 113-0033, Japan*

²*The School of Physics and Astronomy, University of Leeds, Leeds LS2 9JT, UK*

³*Department of Physics, University of Oxford, Clarendon Laboratory, Oxford OX1 3PU, UK*

⁴*CNRS, LTCI, Telecom ParisTech, 37/39 rue Dareau, 75014 Paris, France*

⁵*Institute for Nano Quantum Information Electronics,
The University of Tokyo, Tokyo 113-0033, Japan*

The geometric measure of entanglement is investigated for permutation symmetric pure states of multipartite qubit systems, in particular the question of maximum entanglement. This is done with the help of the Majorana representation, which maps an n qubit symmetric state to n points on the unit sphere. It is shown how symmetries of the point distribution can be exploited to simplify the calculation of entanglement and also help find the maximally entangled symmetric state. Using a combination of analytical and numerical results, the most entangled symmetric states for up to 12 qubits are explored and discussed. The optimization problem on the sphere presented here is then compared with two classical optimization problems on the S^2 sphere, namely Tóth's problem and Thomson's problem, and it is observed that, in general, they are different problems.

PACS numbers: 03.67.Mn, 02.60.Pn, 03.65.Ta, 03.65.Ud, 03.67.Lx

I. INTRODUCTION

Being the fundamental resource in a wide range of situations in quantum information processing, entanglement is considered as a 'standard currency' for quantum information tasks, and it is highly desirable to know which states of a given system exhibit a high or maximal amount of entanglement [1]. When it comes to multipartite states this question becomes complicated. There are different *types* of entanglement [2], alongside which there are many different ways to quantify entanglement, each of which may capture a different desirable quality of a state as a resource.

In this work, the geometric measure of entanglement, a distance-like entanglement measure [3, 4], will be investigated to analyze maximally entangled multipartite states. There are several incentives to consider this particular measure. Firstly, it has a broad range of operational interpretations: for example, in local state discrimination [5], additivity of channel capacities [6] and recently for the classification of states as resources for measurement-based quantum computation (MBQC)[7–9]. Another advantage of the geometric measure is that, while other known entanglement measures are notoriously difficult to compute from their variational definitions, the definition of the geometric measure allows for a comparatively easy calculation. Furthermore, the geometric measure can be linked to other distance-like entanglement measures, such as the robustness of entanglement and the relative entropy of entanglement [4, 10, 11]. The function also has applications in signal processing, particularly in the fields of multi-way

data analysis, high order statistics and independent component analysis (ICA), where it is known under the name *rank one approximation to high order tensors* [12–17].

We focus our attention on permutation-symmetric states – that is, states that are invariant when swapping any pair of particles. This class of states has been useful for different quantum information tasks (for example, in leader election [18]). It includes the Greenberger-Horne-Zeilinger (GHZ) states [19], W states and Dicke states [20], and also occurs in a variety of situations in many-body physics. There has been lots of activity recently in implementing these states experimentally [21, 22]. Furthermore, the symmetric properties make them amenable to the analysis of entanglement properties [10, 23–27].

An important tool in this work will be the Majorana representation [28], a generalization of the Bloch sphere representation of single qubits, where a permutation-symmetric state of n qubits is unambiguously mapped to n points on the surface of the unit sphere. Recently, the Majorana representation has proved very useful in analyzing entanglement properties of symmetric states [23, 26, 27]. In particular, the geometric measure of entanglement has a natural interpretation, and the Majorana representation facilitates exploitation of further symmetries to characterize entanglement [23]. For example, the two-qubit symmetric Bell state $|\psi^+\rangle = 1/\sqrt{2}(|01\rangle + |10\rangle)$ is represented by an antipodal pair of points: the north pole $|0\rangle$ and the south pole $|1\rangle$. Roughly speaking, symmetric states with a high degree of entanglement are represented by point distributions that are well spread out over the sphere. We will use this idea along with other symmetry arguments to look for the most entangled states. Along the way we will compare this problem to other optimization problems of point distributions on the sphere.

The paper is organized as follows. In Section II, the definition and properties of the geometric measure of entanglement are briefly recapitulated, which is followed

* pyma@leeds.ac.uk

† markham@telecom-paristech.fr

‡ murao@phys.s.u-tokyo.ac.jp

by an introduction and discussion of symmetric states in Section III. In Section IV, the Majorana representation of symmetric states is introduced. The problem of finding the maximally entangled state is phrased in this manner, and is compared to two other point distribution problems on S^2 : Tóth's problem and Thomson's problem. In Section V, some theoretical results for symmetric states are derived with the help of the intuitive idea of the Majorana representation. The numerically determined maximally entangled symmetric states of up to 12 qubits are presented in Section VI. Our results are discussed in Section VII, and Section VIII contains the conclusion.

II. THE GEOMETRIC MEASURE OF ENTANGLEMENT

The geometric measure of entanglement is a distance-like entanglement measure for pure multipartite states that assesses the entanglement of a state in terms of its remoteness from the set of separable states [29]. It is defined as the maximal overlap of a given pure state with all pure product states [3, 30, 31] and is also defined as the geodesic distance with respect to the Fubini-Study metric [32]. Here we present it in the inverse logarithmic form of the maximal overlap, which is more convenient in relation to other entanglement measures:

$$E_G(|\psi\rangle) = \min_{|\lambda\rangle \in \mathcal{H}_{\text{SEP}}} \log_2 \left(\frac{1}{|\langle \lambda | \psi \rangle|^2} \right). \quad (1)$$

E_G is non-negative and zero iff $|\psi\rangle$ is a product state. We denote a product state closest to $|\psi\rangle$ by $|\Lambda_\psi\rangle \in \mathcal{H}_{\text{SEP}}$, and it should be noted that a given $|\psi\rangle$ can have more than one closest product state. Indeed, we will usually deal with entangled states that have several closest product states. Due to its compactness, the normalized, pure Hilbert space of a finite-dimensional system (e.g. n qudits) always contains at least one state $|\Psi\rangle$ with maximal entanglement, and to each such state relates at least one closest product state. The task of determining maximal entanglement can be formulated as a max-min problem, with the two extrema not necessarily being unambiguous:

$$\begin{aligned} E_G^{\max} &= \max_{|\psi\rangle \in \mathcal{H}} \min_{|\lambda\rangle \in \mathcal{H}_{\text{SEP}}} \log_2 \left(\frac{1}{|\langle \lambda | \psi \rangle|^2} \right), \\ &= \max_{|\psi\rangle \in \mathcal{H}} \log_2 \left(\frac{1}{|\langle \Lambda_\psi | \psi \rangle|^2} \right), \\ &= \log_2 \left(\frac{1}{|\langle \Lambda_\Psi | \Psi \rangle|^2} \right). \end{aligned} \quad (2)$$

It is often more convenient to define $G(|\psi\rangle) = \max_{|\lambda\rangle} |\langle \lambda | \psi \rangle|$, so that we obtain $E_G = \log_2(1/G^2)$. Because of the monotonicity of this relationship, the task of finding the maximally entangled state is equivalent to solving the min-max problem

$$\min_{|\psi\rangle \in \mathcal{H}} G(|\psi\rangle) = \min_{|\psi\rangle \in \mathcal{H}} \max_{|\lambda\rangle \in \mathcal{H}_{\text{SEP}}} |\langle \lambda | \psi \rangle|. \quad (3)$$

As mentioned in the Introduction, there are several advantages of this measure of entanglement. First of all, it has several operational interpretations. It has implications for channel capacity [6] and can also be used to give conditions as to when states are useful resources for MBQC [7–9]. If the entanglement of a set of resource states scales anything below logarithmically with the number of parties, it cannot be an efficient resource for deterministic universal MBQC [8]. On the other hand, somewhat surprisingly, if the entanglement is too large, it is also not a good resource for MBQC. If the geometric measure of entanglement of an n qubit system scales larger than $n - \delta$ (where δ is some constant), then such a computation can be simulated efficiently computationally [7]. Of course, we should also note that there are many other quantum information tasks that are not restricted by such requirements. For example, the n -qubit GHZ state can be considered the most non-local with respect to all possible two-output, two-setting Bell inequalities [33], whereas the geometric measure is only $E_G(|\text{GHZ}\rangle) = 1$, independent of n . The n -qubit W state, on the other hand, is the optimal state for leader election [18] with entanglement $E_G(|\text{W}\rangle) = \log_2(n/(n-1))^{n-1}$. Indeed, for local state discrimination, the role of entanglement in blocking the ability to access information locally is strictly monotonic – the higher the geometric measure of entanglement, the harder it is to access information locally [5].

In addition, the geometric measure E_G has close links to other distance-like entanglement measures, namely the (global) robustness of entanglement R [34] and the relative entropy of entanglement E_R [29]. Between these measures the inequalities $E_G \leq E_R \leq \log_2(1+R)$ hold for all states [4, 10, 11], and they turn into equalities for stabilizer states (e.g. GHZ state), Dicke states (e.g. W state) and permutation-antisymmetric basis states [5, 10, 35].

An upper bound for the entanglement of pure n qubit states is given in [36] as

$$E_G(|\psi\rangle) \leq n - 1. \quad (4)$$

We can see that this allows for states to be more entangled than is useful, e.g. for MBQC. Indeed, although no states of more than two qubits reach this bound [36], most states of n qubits have entanglement $E_G > n - 2 \log_2(n) - 3$ [7]. In the next section, we will see that symmetric states have generally lower entanglement.

We can also make a general statement for positive states that will help us in calculating entanglement for this smaller class of states. For finite-dimensional systems, a general quantum state can be written in the form $|\psi\rangle = \sum_i a_i |i\rangle$ with an orthonormalized basis $\{|i\rangle\}$ and complex coefficients $a_i \in \mathbb{C}$. We will call $|\psi\rangle$ a *real state* if – for a given basis $\{|i\rangle\}$ – all coefficients are real ($a_i \in \mathbb{R}$), and likewise call $|\psi\rangle$ a *positive state* if the coefficients are all positive ($a_i \geq 0$). A *computational basis* is one made up of tensors of local bases.

Lemma 1. *Every state $|\psi\rangle$ of a finite-dimensional system that is positive with respect to some computational basis has at least one positive closest product state $|\Lambda_\psi\rangle$.*

Proof. Picking any computational basis in which the coefficients of $|\psi\rangle$ are all positive, we denote the basis of subsystem j with $\{|i_j\rangle\}$, and can write the state as $|\psi\rangle = \sum_{\vec{i}} a_{\vec{i}} |i_1\rangle \cdots |i_n\rangle$, with $\vec{i} = (i_1, \dots, i_n)$ and $a_{\vec{i}} \geq 0$. A closest product state of $|\psi\rangle$ can be written as $|\Lambda_\psi\rangle = \bigotimes_j |\sigma_j\rangle$, where $|\sigma_j\rangle = \sum_{i_j} b_{i_j}^j |i_j\rangle$ (with $b_{i_j}^j \in \mathbb{C}$) is the state of subsystem j . Now define a new product state with positive coefficients as $|\Lambda'_\psi\rangle = \bigotimes_j |\sigma'_j\rangle$, where $|\sigma'_j\rangle = \sum_{i_j} |b_{i_j}^j| |i_j\rangle$. Because of $|\langle\psi|\Lambda'_\psi\rangle| = \sum_{\vec{i}} a_{\vec{i}} \prod_j |b_{i_j}^j| \geq \left| \sum_{\vec{i}} a_{\vec{i}} \prod_j b_{i_j}^j \right| = |\langle\psi|\Lambda_\psi\rangle|$, the positive state $|\Lambda'_\psi\rangle$ is a closest product state of $|\psi\rangle$. \square

This lemma, which was also shown in [37], asserts that positive states have at least one positive closest product state, but there can nevertheless exist other non-positive closest product states. A statement analogous to Lemma 1 does not hold for real states, and it is easy to find examples of real states that have no real closest product state.

From now on we will simply denote entanglement instead of referring to the geometric measure of entanglement. It must be kept in mind, however, that the maximally entangled state of a multipartite system subtly depends on the chosen entanglement measure [38].

III. PERMUTATION SYMMETRIC STATES

In general it is very difficult to find the closest product state of a given quantum state, due to the large amount of parameters in $|\Lambda\rangle$. The problem will be considerably simplified, however, when considering permutation-symmetric states. In experiments with many qubits, it is often not possible to access single qubits individually, necessitating a fully symmetrical treatment of the initial state and the system dynamics [39]. The ground state of the Lipkin-Meshkov-Glick model was found to be permutation-invariant, and its entanglement was quantified in term of the geometric measure and its distance-related cousins [40]. For these reasons it is worth analyzing various theoretical and experimental aspects of the entanglement of symmetric states, such as entanglement witnesses or experimental setups [41, 42].

The symmetric basis states of a system of n qubits are given by the Dicke states, the simultaneous eigenstates of the total angular momentum J and its z -component J_z [20, 39, 43]. They are mathematically expressed as the sum of all permutations of computational basis states with $n - k$ qubits being $|0\rangle$ and k being $|1\rangle$.

$$|S_{n,k}\rangle = \binom{n}{k}^{-1/2} \sum_{\text{perm}} \underbrace{|0\rangle|0\rangle \cdots |0\rangle}_{n-k} \underbrace{|1\rangle|1\rangle \cdots |1\rangle}_k, \quad (5)$$

with $0 \leq k \leq n$, and where we omitted the tensor symbols that mediate between the n single qubit spaces. The Dicke states constitute an orthonormalized set of basis vectors for the symmetric Hilbert space \mathcal{H}_s . The notation $|S_{n,k}\rangle$

will sometimes be abbreviated as $|S_k\rangle$ when the number of qubits is clear.

Recently, there has been a very active investigation into the conjecture that the closest product state of a symmetric state is symmetric itself [4, 10, 25]. A proof of this seemingly straightforward statement is far from trivial, and after some special cases were proofed [44, 45], Hübener *et al.* [25] were able to extend this result to the general case. They also showed that, for $n \geq 3$ qudits (general quantum d -level systems) the closest product state of a symmetric state is *necessarily* symmetric. This result greatly reduces the complexity of finding the closest product state and thus the entanglement of a symmetric state.

A general pure symmetric state of n qubits is a linear combination of the $n + 1$ symmetric basis states, with the operational nature being that the state remains invariant under the permutation of any two of its subsystems.

A closest product state of $|S_{n,k}\rangle$ is [10]

$$|\Lambda\rangle = \left(\sqrt{\frac{n-k}{n}} |0\rangle + \sqrt{\frac{k}{n}} |1\rangle \right)^{\otimes n}, \quad (6)$$

i.e. a tensor product of n identical single qubit states. From this, the amount of entanglement is found to be

$$E_G(|S_{n,k}\rangle) = \log_2 \left(\frac{\binom{n}{k}^k \binom{n}{n-k}^{n-k}}{\binom{n}{k}} \right). \quad (7)$$

This formula straightforwardly gives the maximally entangled Dicke state. For even n it is $|S_{n,n/2}\rangle$ and for odd n the two equivalent states $|S_{n,(n+1)/2}\rangle$ and $|S_{n,(n-1)/2}\rangle$. In general, however, the maximally entangled symmetric state of n qubits is a superposition of Dicke states. Nevertheless, Equation (7) can be used as a lower bound to the maximal entanglement of symmetric states. This bound can be approximated by the Stirling formula for large n as $E_G \geq \log_2 \sqrt{n\pi/2}$.

An upper bound to the geometric measure for symmetric n qubit states can be easily found from the well-known decomposition of the identity on the symmetric subspace (denoted $\mathbb{1}_{\text{Symm}}$, see e.g. [46]),

$$\int_{\mathcal{S}(\mathcal{H})} (|\theta\rangle\langle\theta|)^{\otimes n} \omega(\theta) = \frac{1}{n+1} \mathbb{1}_{\text{Symm}}, \quad (8)$$

where ω denotes the uniform probability measure over the unit sphere $\mathcal{S}(\mathcal{H})$ on Hilbert space \mathcal{H} . We can easily see that $G(|\psi\rangle)^2 = \max_{\omega \in \mathcal{H}_{\text{SEP}}} \text{Tr}(\omega|\psi\rangle\langle\psi|) \geq 1/(n+1)$. Hence, for any symmetric state of n qubits, the geometric measure of entanglement is upper bounded by

$$E_G(|\psi\rangle_s) \leq \log_2(n+1). \quad (9)$$

An alternative proof that has the benefit of being visually accessible is presented in Appendix A.

The maximal symmetric entanglement for n qubits thus scales polylogarithmically between $\mathcal{O}(\log \sqrt{n})$ and $\mathcal{O}(\log n)$. To compare this with the general non-symmetric case, consider the lower bound of the maximal n

qubit entanglement (n even) of $E_G \geq (n/2)$ [47]. Thus the maximal entanglement of general states scales much faster, namely linearly rather than logarithmically. As mentioned, for most states the entanglement is even higher and thus too entangled to be useful for MBQC. While the bounds for symmetric states mean that permutation-symmetric states are never too entangled to be useful for MBQC, unfortunately their scaling is also too low to be good universal deterministic resources [8]. They may nevertheless be candidates for approximate, stochastic MBQC [9]. Regardless of their use as resources for MBQC, the comparatively high entanglement of symmetric states still renders them formidable candidates for specific quantum computations or as resources for other tasks, such as the leader election problem [18] and LOCC discrimination [5].

We end this section by mentioning a simplification with respect to symmetric positive states. States that are symmetric as well as positive in some computational basis are labelled as *positive symmetric*. From the previous discussion it is clear that such states have a closest product state which is positive symmetric itself, a result first shown in [10]. It should be noted that, while each closest product state of a positive symmetric state is *necessarily* symmetric for $n \geq 3$ qudits, it *need not* be positive. We can formulate this as a statement akin to Lemma 1.

Lemma 2. *Every symmetric state $|\psi\rangle_s$ of n qudits, which is positive in some computational basis, has at least one positive symmetric closest product state $|\Lambda_\psi\rangle_s$.*

IV. MAJORANA REPRESENTATION OF SYMMETRIC STATES

With the discussion of the geometric measure and symmetric states behind us, we have gathered the prerequisites to introduce a crucial tool, the Majorana representation. It will help us to understand the amount of entanglement of symmetric states.

A. Definition

In classical physics, the angular momentum \mathbf{J} of a system can be represented by a point on the surface of the 3D unit sphere S^2 , which corresponds to the direction of \mathbf{J} . No such simple representation is possible in quantum mechanics, but Majorana [28] pointed out that a pure state of spin- j can be uniquely represented by $2j$ not necessarily distinct points on S^2 . This is a generalization of the spin-1/2 (qubit) case, where the 2D Hilbert space is isomorphic to the unit vectors on the Bloch sphere.

An equivalent representation also exists for permutation-symmetric states of n spin-1/2 particles [28, 48]. By means of this ‘Majorana representation’ any symmetric state of n qubits $|\psi\rangle_s$ can be uniquely composed from a sum over all permutations $P: \{1, \dots, n\} \rightarrow \{1, \dots, n\}$

of n undistinguishable single qubit states $\{|\phi_1\rangle, \dots, |\phi_n\rangle\}$:

$$|\psi\rangle_s = \frac{1}{\sqrt{K}} \sum_{\text{perm}} |\phi_{P(1)}\rangle |\phi_{P(2)}\rangle \cdots |\phi_{P(n)}\rangle, \quad (10)$$

$$\text{with } |\phi_i\rangle = \cos \frac{\theta_i}{2} |0\rangle + e^{i\varphi_i} \sin \frac{\theta_i}{2} |1\rangle,$$

$$\text{and } K = n! \sum_{\text{perm}} \prod_{i=1}^n \langle \phi_i | \phi_{P(i)} \rangle.$$

The normalization factor K is in general different for different $|\psi\rangle_s$. By means of Equation (10), the multi-qubit state $|\psi\rangle_s$ can be visualized by n unordered points (each of which has a Bloch vector pointing in its direction) on the surface of a sphere. We call these points the *Majorana points* (MP), and the sphere on which they lie the *Majorana sphere*.

With Equation (10), the form of a symmetric state $|\psi\rangle_s$ can be explicitly determined if the MPs are known. If the MPs of a given state $|\psi\rangle_s = \sum_{k=0}^n a_k |S_k\rangle$ are unknown, they can be determined by solving a system of $n+1$ equations.

$$a_k = \binom{n}{k}^{1/2} \sum_{\text{perm}} S_{P(1)} \cdots S_{P(k)} C_{P(k+1)} \cdots C_{P(n)}, \quad (11)$$

$$\text{with } C_i = \cos \frac{\theta_i}{2}, \quad S_i = e^{i\varphi_i} \sin \frac{\theta_i}{2}.$$

The Majorana representation has been rediscovered several times, and has been put to many different uses across physics. In relation to the foundations of quantum mechanics, it has been used to find efficient proofs of the Kochen-Specker theorem [49, 50] and to study the ‘quantumness’ of pure quantum states in several respects [51, 52], as well as the approach to classicality in terms of the discriminability of states [53]. It has also been used to study Berry phases in high spin [54] and quantum chaos [55, 56]. Within many-body physics it has been used for finding solutions to the Lipkin-Meshkov-Glick model [57], and for studying and identifying phases in spinor BEC [58–61]. It has also been used to look for optimal resources for reference frame alignment [62] and for phase estimation [63].

Recently, the Majorana representation has also become a useful tool in studying the entanglement of permutation-symmetric states. It has been used to search for and characterize different classes of entanglement [23, 26, 27], which have interesting mirrors in the classification of phases in spinor condensates [23, 59]. Of particular interest, in this work, is that it gives a natural visual interpretation of the geometric measure of entanglement [23], and we will see how symmetries in the point distributions can be used to calculate the entanglement and assist in finding the most entangled states.

The connection to entanglement can first be noticed by the fact that the point distribution is invariant under local unitary maps. Applying an arbitrary single-qubit unitary operation U to each of the n subsystems yields the LU map

$$|\psi\rangle_s \longmapsto |\varphi\rangle_s \equiv U \otimes \cdots \otimes U |\psi\rangle_s, \quad (12)$$

and from Equation (10) it follows that

$$|\varphi\rangle_s = \frac{1}{\sqrt{K}} \sum_{\text{perm}} |\vartheta_{P(1)}\rangle |\vartheta_{P(2)}\rangle \cdots |\vartheta_{P(n)}\rangle, \quad (13)$$

with $|\vartheta_i\rangle = U|\phi_i\rangle \forall i$.

In other words, the symmetric state $|\psi\rangle_s$ is mapped to another symmetric state $|\varphi\rangle_s$, and the MP distribution of $|\varphi\rangle_s$ is obtained by a joint rotation of the MP distribution of $|\psi\rangle_s$ on the Majorana sphere along a common axis. Therefore $|\psi\rangle_s$ and $|\varphi\rangle_s$ have different MPs, but the same *relative* distribution of the MPs, and the entanglement remains unchanged.

When it comes to the geometric measure of entanglement, we can be even more precise. For $n \geq 3$ qubits, every closest product state $|\Lambda\rangle_s$ of a symmetric state $|\psi\rangle_s$ is symmetric itself [25], so that one can write $|\Lambda\rangle_s = |\sigma\rangle^{\otimes n}$ with a single qubit state $|\sigma\rangle$, and visualize $|\Lambda\rangle_s$ by the Bloch vector of $|\sigma\rangle$. In analogy to the Majorana points, we refer to $|\sigma\rangle$ as a *closest product point* (CPP).

For the calculation of the geometric measure of entanglement, the overlap with a symmetric product state $|\lambda\rangle = |\sigma\rangle^{\otimes n}$ is

$$|\langle \lambda | \psi \rangle_s| = \frac{n!}{\sqrt{K}} \prod_{i=1}^n |\langle \sigma | \phi_i \rangle|. \quad (14)$$

The task of determining the CPP of a given symmetric state is thus equivalent to maximizing the absolute value of a product of scalar products. From a geometrical point of view, the $\langle \sigma | \phi_i \rangle$ are the angles between the two corresponding points on the Majorana sphere, and thus the determination of the CPP can be viewed as an optimization problem for a product of geometrical angles.

B. Examples

We will now demonstrate the Majorana representation for two and three qubit symmetric states. The case of two qubits is very simple, because any distribution of two points can be rotated on the Majorana sphere in a way that both MPs are positive, with $|\phi_1\rangle = |0\rangle$ and $|\phi_2\rangle = \cos \frac{\theta}{2} |0\rangle + \sin \frac{\theta}{2} |1\rangle$ for some $\theta \in [0, \pi]$. One CPP of this MP distribution is easily found to be $|\sigma\rangle = \cos \frac{\theta}{4} |0\rangle + \sin \frac{\theta}{4} |1\rangle$. Figure 1 shows two examples for $\theta = \pi/2$ and $\theta = \pi$, with the latter representing the Bell state $|\psi^+\rangle = 1/\sqrt{2}(|01\rangle + |10\rangle)$. Due to the azimuthal symmetry of its MPs on the sphere, the CPPs form a continuous ring $|\sigma\rangle = 1/\sqrt{2}(|0\rangle + e^{i\varphi}|1\rangle)$, with $\varphi \in [0, 2\pi)$ around the equator. The amount of entanglement is $E_G(|\psi^+\rangle) = 1$. For two qubits, the maximally entangled symmetric states are easily found to be those whose MPs lie diametrically opposite on the sphere.

For three qubit states, the GHZ state and the W state, both of which are positive and symmetric, are considered as extremal among three qubit states [64]. The tripartite

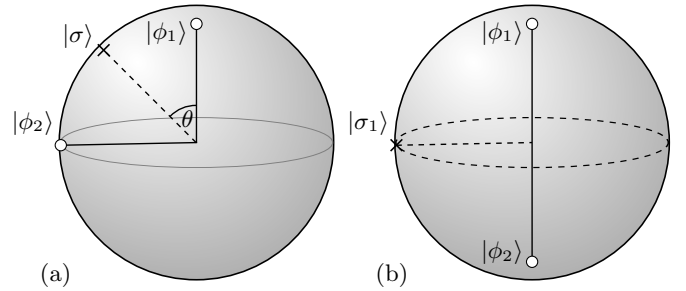


FIG. 1. The Majorana representations of two symmetric states of two qubits. MPs are shown as white circles and CPPs as dashed lines or crosses. Panel (a) depicts the state $\sqrt{2/3}|00\rangle + \sqrt{1/6}(|01\rangle + |10\rangle)$. Its single CPP lies in the middle of the two MPs at an angle of $\theta = \pi/4$. Panel (b) shows the Bell state $|\psi^+\rangle = 1/\sqrt{2}(|01\rangle + |10\rangle)$, whose CPPs form a continuous ring on the equatorial belt.

GHZ state $|\text{GHZ}\rangle = 1/\sqrt{2}(|000\rangle + |111\rangle)$ [19] has the MPs

$$\begin{aligned} |\phi_1\rangle &= \frac{1}{\sqrt{2}}(|0\rangle + |1\rangle), \\ |\phi_2\rangle &= \frac{1}{\sqrt{2}}(|0\rangle + e^{i2\pi/3}|1\rangle), \\ |\phi_3\rangle &= \frac{1}{\sqrt{2}}(|0\rangle + e^{i4\pi/3}|1\rangle). \end{aligned} \quad (15)$$

Its two CPPs are easily calculated to be $|\sigma_1\rangle = |0\rangle$ and $|\sigma_2\rangle = |1\rangle$, yielding an entanglement of $E_G(|\text{GHZ}\rangle) = 1$. Figure 2(a) shows the distribution of the MPs and CPPs for the GHZ state. The three MPs form an equilateral triangle inside the equatorial belt, and the two CPPs lie at the north and the south pole, respectively.

The W state $|\text{W}\rangle = |S_{3,1}\rangle = 1/\sqrt{3}(|001\rangle + |010\rangle + |100\rangle)$ is a Dicke state, and its MPs can be immediately accessed from its form as

$$\begin{aligned} |\phi_1\rangle &= |\phi_2\rangle = |0\rangle, \\ |\phi_3\rangle &= |1\rangle. \end{aligned} \quad (16)$$

Generally, the definition (5) of the Dicke states $|S_{n,k}\rangle$ asserts that $n - k$ MPs lie at the north pole and k at

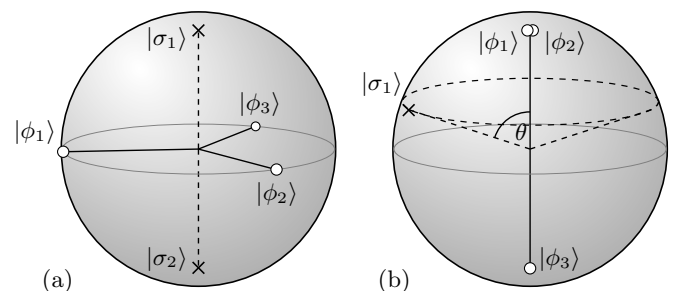


FIG. 2. The MPs and CPPs of the three qubit (a) GHZ state and (b) W state. The GHZ state has two discrete CPPs whereas for the W state the CPPs form a continuous ring due to the azimuthal symmetry.

the south pole. Equation (6) yields $|\sigma_1\rangle = \sqrt{2/3}|0\rangle + \sqrt{1/3}|1\rangle$ as a positive CPP of the W state, and from the azimuthal symmetry of the MP distribution it is clear that the set of all CPPs is formed by the ring of vectors $|\sigma\rangle = \sqrt{2/3}|0\rangle + e^{i\varphi}\sqrt{1/3}|1\rangle$, with $\varphi \in [0, 2\pi)$. Figure 2(b) shows the MPs and CPPs of $|W\rangle$. The amount of entanglement is $E_G(|W\rangle) = \log_2(9/4) \approx 1.17$, which is higher than that of the GHZ state. It was recently shown that, in terms of the geometric measure, the W state is the maximally entangled of all three qubit states [65].

It is insightful to examine how the CPPs and the entanglement change when the MP distribution of the underlying state is modified. Starting out with three MPs lying on the north pole, two of the MPs are moved southwards on opposite sides (cf. Figure 3), describing an isosceles triangle with the remaining MP on the north pole. Using the abbreviations $c_\theta = \cos(\theta/2)$ and $s_\theta = \sin(\theta/2)$, the MPs have the form

$$\begin{aligned} |\phi_1\rangle &= |0\rangle, \\ |\phi_{2,3}\rangle &= c_\theta|0\rangle \pm i s_\theta|1\rangle, \end{aligned} \quad (17)$$

with the parametrization $\theta \in [0, \pi]$. The form of the underlying quantum state follows from Equation (10) as

$$|\psi\rangle = \frac{3c_\theta^2|000\rangle + s_\theta^2(|011\rangle + |101\rangle + |110\rangle)}{\sqrt{9c_\theta^4 + 3s_\theta^4}}. \quad (18)$$

This state is positive, so Lemma 2 asserts the existence of at least one positive CPP. With the ansatz $|\sigma\rangle =$

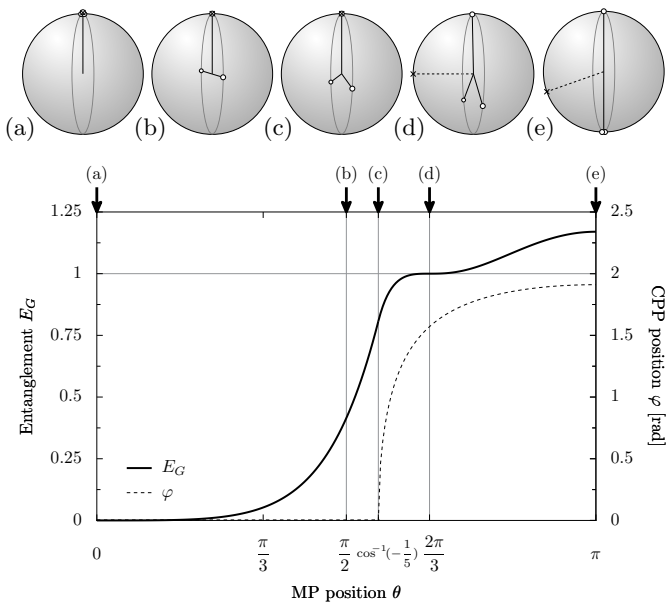


FIG. 3. Change of the entanglement and the location of the CPP when the MP distribution is modified. The position of the CPP does not change until the two moving MPs have reached a latitude slightly below the equator. From the distribution (c) onwards, the CPP rapidly moves southwards and reaches the equator at the GHZ state (d). After that, the location of the CPP and the entanglement changes only weakly until the W state (e) is reached.

$c_\varphi|0\rangle + s_\varphi|1\rangle$ for the CPP, the position of the CPP is found by calculating the absolute maximum of $|\langle\psi|\sigma\rangle|^{\otimes 3}$. From this it is found that the parameter $\varphi(\theta)$ of the CPP depends on the parameter θ of the MPs as follows:

$$c_\varphi^2 = s_\theta^2 / (6s_\theta^2 - 3). \quad (19)$$

The permitted values of the left-hand side are $[0, 1]$, but the right-hand side lies outside this range for $\theta < \pi - \arccos(1/5)$. For these values the CPP is fixed at $|\sigma\rangle = |0\rangle$. Figure 3 shows how the CPP parameter $\varphi(\theta)$ changes with θ . It is seen that from $\theta = \pi - \arccos(1/5)$ onwards, the CPP abruptly leaves the north pole and moves towards the south pole along the prime meridian. From Equations (18) and (19) the amount of entanglement is easily calculated and is displayed in Figure 3. E_G is monotonously increasing [64] and reaches a saddle point at the GHZ state ($\theta = 2\pi/3$).

C. Entanglement and extremal point distributions

The main point of interest in this paper is the study of maximally entangled symmetric states. For this the Majorana representation is extremely helpful, because it allows the optimization problem of maximizing the entanglement to be written in a simple form. With the help of Equation (14), the min-max problem (3) for finding the maximally entangled state can be reformulated as

$$\min_{\{|\phi_i\rangle\}} \frac{1}{\sqrt{K}} \left(\max_{|\sigma\rangle} \prod_{i=1}^n |\langle\sigma|\phi_i\rangle| \right). \quad (20)$$

This ‘Majorana problem’ bears all the properties of an optimization problem on the surface of a sphere in \mathbb{R}^3 . These kinds of problems deal with arrangements of a finite number of points on a sphere so that an extremal property is fulfilled [66]. Two well-known members, Tóth’s problem and Thomson’s problem, have been extensively studied in the past.

Tóth’s problem, also known as Fejes’ problem and Tammes’ problem, asks how n points have to be distributed on the unit sphere so that the minimum distance of all pairs of points becomes maximal [66]. This problem was first raised by the biologist Tammes in 1930 when trying to explain the observed distribution of pores on pollen grains [67]. Recasting the n points as unit vectors $\mathbf{r}_i \in \mathbb{R}^3$, the following cost function needs to be maximized:

$$f_{\text{Tóth}}(\mathbf{r}_1, \mathbf{r}_2, \dots, \mathbf{r}_n) = \min_{i < j} |\mathbf{r}_i - \mathbf{r}_j|. \quad (21)$$

The point configuration that solves this problem is called a spherical code or sphere packing [68]. The latter term refers to the equivalent problem of placing n identical spheres of maximal possible radius around a central unit sphere, touching the unit sphere at the points that solve Tóth’s problem.

Thomson’s problem, also known as the Coulomb problem, asks how n point charges can be distributed

on the surface of a sphere so that the potential energy is minimized. The charges interact with each other only through Coulomb's inverse square law. Devised by J. J. Thomson in 1904, this problem raises the question about the stable patterns of up to 100 electrons on a spherical surface [69]. Its cost function is given by the Coulomb energy and needs to be minimized.

$$f_{\text{Thomson}}(\mathbf{r}_1, \mathbf{r}_2, \dots, \mathbf{r}_n) = \sum_{i < j} |\mathbf{r}_i - \mathbf{r}_j|^{-1} . \quad (22)$$

The original motivation for Thomson's problem was to determine the stable electron distribution of atoms in the plum pudding model. While this model has been superseded by modern quantum theory, there is a wide array of novel applications for Thomson's problem or its generalization to other interaction potentials. Among these are multi-electron bubbles in liquid ^4He [70], surface ordering of liquid metal drops confined in Paul traps [71], the shell structure of spherical viruses [72], 'colloidosomes' for encapsulating biochemically active substances [73], fullerene patterns of carbon atoms [74] and the Abrikosov lattice of vortices in superconducting metal shells [75].

Exact solutions to Tóth's problem are only known for $n_{\text{To}} = 2 - 12, 24$ points [76], and in Thomson's problem for $n_{\text{Th}} = 2 - 8, 12$ points [66, 76]. Despite the different definitions of the two problems, they share the same solutions for $n = 2 - 6, 12$ points [77]. Numerical solutions are, furthermore, known for a wide range of n in both problems [78–81].

The solutions to $n = 2, 3$ are trivial and given by the dipole and equilateral triangle, respectively. For $n = 4, 6, 8, 12, 20$ the Platonic solids are natural candidates, but they are the actual solutions only for $n = 4, 6, 12$ [82]. For $n = 8, 20$ the solutions are not Platonic solids and are different for the two problems. We will cover the solutions for $n = 4 - 12$ in more detail alongside the Majorana problem in Section VI.

On symmetry grounds, one could expect that the center of mass of the n points always coincides with the sphere's middle point. This is, however, not the case, as the solution to Tóth's problem for $n = 7$ [76] or the solution to Thomson's problem for $n = 11$ shows [76, 78]. Furthermore, the solutions need not be unique. For Tóth's problem, the first incident of this is $n = 5$ [83], and for Thomson's problem at $n = 15$ [76] and $n = 16$ [78]. These aspects show that it is, in general, hard to make statements about the form of the 'most spread out' point distributions on the sphere. The Majorana problem (20) is considered to be equally tricky, particularly with the normalization factor K depending on the MPs. Furthermore, the MPs of the solution need not all be spread out far from each other, as demonstrated by the three qubit $|\text{W}\rangle$ state with its two coinciding MPs.

V. STATES AND SYMMETRIES OF MP AND CPP DISTRIBUTIONS

In this section, results for the interdependence between the form of n qubit symmetric states and their Majorana representation will be derived. More specifically, it will be examined what the distributions of MPs and CPPs look like for states whose coefficients are real, positive or vanishing. In some of these cases the MPs or CPPs have distinct patterns on the sphere, which can be described by symmetries. In this context, care has to be taken as to the meaning of the word 'symmetric'. Permutation-symmetric states were introduced in Section III, and only these states can be represented by point distributions on the Majorana sphere. For some of these symmetric states, their MP distribution exhibits symmetry properties on the sphere. Examples of this can be found in Figure 2, where the GHZ state and W state have *rotational symmetries* around the Z-axis, as well as *reflective symmetries* along some planes.

Let $|\psi\rangle_s = \sum_{k=0}^n a_k |S_k\rangle$ be a general symmetric state of n qubits. To understand the relationship between the state's coefficients and the Majorana representation, consider the effect of symmetric LUs. A symmetric LU acting on the Hilbert space of an n qubit system is defined as the n -fold tensor product of a single-qubit unitary operation: $U^s = U \otimes \dots \otimes U$. This is precisely the LU map that was shown in Equation (12) and (13) to map every symmetric state to another symmetric state.

Considering the Hilbert space of a single qubit, the rotation operator for Z-axis rotations of the qubit is

$$R_z(\theta) = \begin{pmatrix} 1 & 0 \\ 0 & e^{i\theta} \end{pmatrix} , \quad (23)$$

and the rotation operator for Y-axis rotations of the qubit is

$$R_y(\theta) = \begin{pmatrix} \cos \frac{\theta}{2} & -\sin \frac{\theta}{2} \\ \sin \frac{\theta}{2} & \cos \frac{\theta}{2} \end{pmatrix} . \quad (24)$$

R_z changes the relative phase, but not the absolute value of the qubit's coefficients. Conversely, R_y changes the absolute value, but not the relative phase of the coefficients. From Equation (10) it is easily seen that R_z and R_y pass this behavior on to the symmetric LUs $R_z^s := R_z^{\otimes n}$ and $R_y^s := R_y^{\otimes n}$. For example, the effect of R_z^s on $|\psi\rangle_s$ is

$$R_z^s(\theta) |\psi\rangle_s = \sum_{k=0}^n a_k e^{ik\theta} |S_k\rangle . \quad (25)$$

From this it is easy to determine the conditions for the MPs of $|\psi\rangle_s$ having a rotational symmetry around the Z-axis, i.e. $R_z^s(\theta) |\psi\rangle_s = |\psi\rangle_s$ (up to a global phase) for some $\theta < 2\pi$. From Equation (25) it is clear that the possible rotational angles (up to multiples) are restricted to $\theta = 2\pi/m$, with $m \in \mathbb{N}$, $1 < m \leq n$. The necessary and sufficient conditions are:

Lemma 3. *The MP distribution of a symmetric n qubit state $|\psi\rangle_s$ is rotationally symmetric around the Z -axis with rotational angle $\theta = 2\pi/m$ ($1 < m \leq n$) iff*

$$\forall\{k_i, k_j | a_{k_i} \neq 0 \wedge a_{k_j} \neq 0\} : (k_i - k_j) \bmod m = 0 \quad (26)$$

Proof. Equation (26) is equivalent to: $\exists l \in \mathbb{Z} : \forall\{k | a_k \neq 0\} : k \bmod m = l$. From this it follows that $R_z^s(2\pi/m)|\psi\rangle_s = \sum_k a_k \exp(i2\pi k/m)|S_k\rangle = \sum_k a_k \exp(i2\pi l/m)|S_k\rangle = e^{i\delta}|\psi\rangle_s$, with $\delta = 2\pi l/m$. \square

In other words, a sufficient number of coefficients need to vanish, and the spacings between the remaining coefficients must be multiples of m . For example, a symmetric state of the form $|\psi\rangle_s = a_3|S_3\rangle + a_7|S_7\rangle + a_{15}|S_{15}\rangle$ is rotationally symmetric with $\theta = \pi/2$, because the spacings between non-vanishing coefficients are multiples of 4.

Lemma 4. *Every maximally entangled symmetric state $|\Psi\rangle_s$ of n qubits has at least two different CPPs.*

Proof. The cases $n = 2, 3$ are trivial, because their maximally entangled states (Bell states and W state, respectively) have an infinite number of CPPs. For $n > 3$, we consider a symmetric state $|\psi\rangle$ with only one CPP $|\sigma\rangle$ and show that $|\psi\rangle$ cannot be maximally entangled.

Because of the LU invariance on the Majorana sphere (cf. Equation (13)), we can take the CPP to be the north pole, i.e. $|\sigma\rangle = |0\rangle$. Denoting a single qubit with $|\omega\rangle = c_\theta|0\rangle + e^{i\varphi}s_\theta|1\rangle$, the smooth and continuous overlap function $g(|\omega\rangle) = |\langle\psi|\omega\rangle^{\otimes n}|$ then has its absolute maximum at $|\omega\rangle = |0\rangle$. For any other local maximum $|\omega'\rangle$, the value of $g(|\omega'\rangle)$ is smaller than $g(|0\rangle)$ and therefore an infinitesimal change in the MPs of $|\psi\rangle$ cannot lead to a CPP outside a small neighborhood of the north pole.

We will now present an explicit variation of $|\psi\rangle$ that increases the entanglement. $|\psi\rangle = \sum_{k=0}^n a_k|S_k\rangle$ has complex coefficients that fulfil $\langle\psi|\psi\rangle = 1$, as well as $a_0 > 0$ and $a_1 = 0$ [84]. Define the variation as $|\psi_\epsilon\rangle = (a_0 - \epsilon)|S_0\rangle + \sum_{k=2}^{n-1} a_k|S_k\rangle + (a_n + \epsilon a_0/a_n^*)|S_n\rangle$, with $\epsilon \ll 1$. This state fulfils the requirement $|\psi_\epsilon\rangle \xrightarrow{\epsilon \rightarrow 0} |\psi\rangle$, and is normalized: $\langle\psi_\epsilon|\psi_\epsilon\rangle = 1 + \mathcal{O}(\epsilon^2)$. We now investigate the values of $g_\epsilon(|\omega\rangle) = |\langle\psi_\epsilon|\omega\rangle^{\otimes n}|$ around the north pole. In this area $|\omega\rangle = (1 - (\theta^2/8) + \mathcal{O}(\theta^4))|0\rangle + e^{i\varphi}((\theta/2) - \mathcal{O}(\theta^3))|1\rangle$, hence $g_\epsilon(|\omega\rangle) = |(1 - (\theta^2/8))^n (a_0 - \epsilon) + \mathcal{O}(\epsilon^2, \theta^2)| = |a_0 - \epsilon| + \mathcal{O}(\epsilon^2, \theta^2) < |a_0| = g(|0\rangle)$ for small, but nonzero ϵ and θ . Therefore the absolute maximum of g_ϵ is smaller than that of g , and $|\psi_\epsilon\rangle$ is more entangled than $|\psi\rangle$. \square

A. Real symmetric states

For symmetric states with real coefficients, the following lemma asserts a reflection symmetry of the MPs and CPPs with respect to the X - Z -plane that cuts the Majorana sphere in half. In mathematical terms, the MPs and CPPs exhibit a reflection symmetry with respect to the X - Z -plane iff for each MP $|\phi_i\rangle = c_\theta|0\rangle + e^{i\varphi}s_\theta|1\rangle$ the complex conjugate point $|\phi_i\rangle^* = c_\theta|0\rangle + e^{-i\varphi}s_\theta|1\rangle$ is also a MP, and the same holds for CPPs too.

Lemma 5. *Let $|\psi\rangle_s$ be a symmetric state of n qubits. $|\psi\rangle_s$ is real iff all its MPs are reflective symmetric with respect to the X - Z -plane of the Majorana sphere.*

Proof. (\Rightarrow) Let $|\psi\rangle_s$ be a real state. Then $|\psi\rangle_s = |\psi\rangle_s^*$, and since Majorana representations are unique, $|\psi\rangle_s$ has the same MPs as $|\psi\rangle_s^*$. Therefore the complex conjugate $|\phi_i\rangle^*$ of each non-real MP $|\phi_i\rangle$ is also a MP.

(\Leftarrow) Let the MPs of $|\psi\rangle_s$ be symmetric with respect to the X - Z -plane. Then for every nonreal MP $|\phi_i\rangle$ its complex conjugate $|\phi_i\rangle^*$ is also a MP. Because $(|\phi_i\rangle|\phi_i\rangle^* + |\phi_i\rangle^*|\phi_i\rangle)$ is real, it becomes clear, from the permutation over all MPs in Equation (10), that the overall state $|\psi\rangle_s$ is real, too. \square

The reflective symmetry of the MPs naturally leads to the same symmetry for the CPPs.

Corollary 1. *Let $|\psi\rangle_s$ be a symmetric state of n qubits. If $|\psi\rangle_s$ is real, then all its CPPs are reflective symmetric with respect to the X - Z -plane of the Majorana sphere.*

Proof. Lemma 5 asserts that for every MP $|\phi_i\rangle$ of $|\psi\rangle_s$, the complex conjugate $|\phi_i\rangle^*$ is also a MP. By considering the complex conjugate of the optimization problem (20), it becomes clear that for any CPP $|\sigma\rangle$ the complex conjugate $|\sigma\rangle^*$ is also a CPP. \square

B. Positive symmetric states

For symmetric states with positive coefficients, strong results can be obtained with regard to the number and locations of the CPPs. In particular, for non-Dicke states it is shown that there are at most $2n - 4$ CPPs and that non-positive CPPs can only exist if the MP distribution has a rotational symmetry around the Z -axis. Furthermore, the CPPs can only lie at specified azimuthal angles on the sphere, namely those that are ‘projected’ from the meridian of positive Bloch vectors by means of the Z -axis rotational symmetry (see, e.g., the positive seven qubit state shown in Figure 7).

Dicke states constitute a special case due to their continuous azimuthal symmetry. The two Dicke states $|S_0\rangle$ and $|S_n\rangle$ are product states, with all their MPs and CPPs lying on the north and the south pole, respectively. For any other Dicke state $|S_k\rangle$ the MPs are shared between the two poles, and the CPPs form a continuous horizontal ring with inclination $\theta = 2 \arccos \sqrt{(n-k)/n}$.

Lemma 6. *Let $|\psi\rangle_s$ be a positive symmetric state of n qubits, excluding the Dicke states.*

- (a) *If $|\psi\rangle_s$ is rotationally symmetric around the Z -axis with minimal rotational angle $2\pi/m$, then all its CPPs $|\sigma(\theta, \varphi)\rangle = c_\theta|0\rangle + e^{i\varphi}s_\theta|1\rangle$ are restricted to the m azimuthal angles given by $\varphi = \varphi_r = 2\pi r/m$ with $r \in \mathbb{Z}$. Furthermore, if $|\sigma(\theta, \varphi_r)\rangle$ is a CPP for some r , then it is also a CPP for all other values of r .*

- (b) If $|\psi\rangle_s$ is not rotationally symmetric around the Z-axis, then all its CPPs are positive.

Proof. The proof runs similar to the one of Lemma 1, where the existence of at least one positive CPP is established. We use the notations $|\psi\rangle_s = \sum_k a_k |S_k\rangle$ with $a_k \geq 0$, and $|\lambda\rangle = |\sigma\rangle^{\otimes n}$.

Case (a): Consider a non-positive CPP $|\sigma\rangle = c_\theta|0\rangle + e^{i\varphi}s_\theta|1\rangle$ with $\varphi = 2\pi r/m$ and $r \in \mathbb{R}$, and define $|\tilde{\sigma}\rangle = c_\theta|0\rangle + s_\theta|1\rangle$. Then $|\langle\lambda|\psi\rangle_s| = |\sum_k e^{ik\varphi} a_k c_\theta^{n-k} s_\theta^k \sqrt{n/k}| \leq \sum_k a_k c_\theta^{n-k} s_\theta^k \sqrt{n/k} = |\langle\tilde{\lambda}|\psi\rangle_s|$. If this inequality is strict, then $|\sigma\rangle$ is not a CPP. This would be a contradiction, so it must be an equality. Thus, for any two indices k_i and k_j of non-vanishing coefficients a_{k_i} and a_{k_j} , the following must hold: $e^{ik_i\varphi} = e^{ik_j\varphi}$. This can be reformulated as $k_i r \bmod m = k_j r$, or equivalently

$$(k_i - k_j) r \bmod m = 0 . \quad (27)$$

Because $\varphi = 2\pi/m$ is the minimal rotational angle, m is the largest integer that satisfies Equation (26), and thus there exist k_i and k_j with $a_{k_i}, a_{k_j} \neq 0$ s.t. $k_i - k_j = m$. From this and from Equation (27), it follows that $r \in \mathbb{Z}$. Therefore $|\sigma(\theta, \varphi_r)\rangle$ is a CPP if and only if r is an integer.

Case (b): Considering a CPP $|\sigma\rangle = c_\theta|0\rangle + e^{i\rho}s_\theta|1\rangle$ with $\rho = 2\pi r$ and $r \in \mathbb{R}$, we need to show that $r \in \mathbb{Z}$. Defining $|\tilde{\sigma}\rangle = c_\theta|0\rangle + s_\theta|1\rangle$, and using the same line of argumentation as above, the equation $e^{ik_i\rho} = e^{ik_j\rho}$ must hold for any pair of non-vanishing a_{k_i} and a_{k_j} . This is equivalent to

$$(k_i - k_j) r \bmod 1 = 0 , \quad (28)$$

or $(k_i - k_j) r \in \mathbb{Z}$, in particular $r \in \mathbb{Q}$. If there exist indices k_i and k_j of non-vanishing coefficients s.t. $k_i - k_j = 1$, then $r \in \mathbb{Z}$, as desired. Otherwise consider $r = x/y$ with coprime $x, y \in \mathbb{N}$, $x < y$. Because $|\psi\rangle_s$ is not rotationally symmetric, the negation of Lemma 3 yields that, for any two k_i and k_j ($a_{k_i}, a_{k_j} \neq 0$) with $k_i - k_j = \alpha > 1$, there must exist a different pair k_p and k_q ($a_{k_p}, a_{k_q} \neq 0$) with $k_p - k_q = \beta > 1$ s.t. α is not a multiple of β and vice versa. From $r = x/y$ and Equation (28), it follows that $y = \alpha$ as well as $y = \beta$. This is a contradiction, so $r \in \mathbb{Z}$. \square

With this result about the confinement of the CPPs to certain azimuthal angles, it is possible to derive upper bounds on the number of CPPs.

Theorem 1. *The Majorana representation of every positive symmetric state $|\psi\rangle_s$ of n qubits, excluding the Dicke states, belongs to one of the following three mutually exclusive classes.*

- (a) $|\psi\rangle_s$ is rotationally symmetric around the Z-axis, with only the two poles as possible CPPs.
- (b) $|\psi\rangle_s$ is rotationally symmetric around the Z-axis, with at least one CPP being non-positive.
- (c) $|\psi\rangle_s$ is not rotationally symmetric around the Z-axis, and all CPPs are positive.

Regarding the CPPs of states from class (b) and (c), the following assertions can be made for $n \geq 3$:

- (b) If both poles are occupied by at least one MP each, then there are at most $2n - 4$ CPPs, else there are at most n CPPs.
- (c) There are at most $\lceil \frac{n+2}{2} \rceil$ CPPs [85].

Proof. Starting with the first part of the theorem, case (c) has already been shown in Lemma 6, so consider states $|\psi\rangle_s$ with a rotational symmetry $\varphi = 2\pi/m$ around the Z-axis. If all CPPs are either $|0\rangle$ or $|1\rangle$, then we have case (a), otherwise there is at least one CPP $|\sigma\rangle$ which does not lie on a pole. If this $|\sigma\rangle$ is non-positive, then we have case (b), and if $|\sigma\rangle$ is positive, then Lemma 6 states the existence of another, non-positive CPP, thus again resulting in case (b).

The proof of the second part of the theorem is a bit involved and can be found in Appendix B. \square

VI. NUMERICAL SOLUTIONS FOR UP TO TWELVE QUBITS

In this section, we present the numerically determined solutions of the Majorana problem for up to 12 qubits. In order to find these, the results from the previous sections were extremely helpful. This is because an exhaustive search over the set of all symmetric states quickly becomes unfeasible, even for low numbers of qubits and because the min-max problem (20) is too complex to allow for straightforward analytic solutions.

Among the results particularly helpful for our search are Lemma 6 and Theorem 1. For positive states they strongly restrict the possible locations of CPPs, and thus greatly simplify the calculation of the entanglement. It then suffices to determine only the positive CPPs because all other CPPs automatically follow from the Z-axis symmetry (if any exists). We will see that this result is especially powerful for the Platonic solids in the cases $n = 4, 6$ where the location of the CPPs can be immediately determined from this argument alone, without the need to do any calculations.

From the definition (2) of E_G , it is clear that the exact amount of entanglement of a given state (or its corresponding MP distribution) is automatically known once the location of at least one CPP is known. A numerical search over the set of positive symmetric states often detects the maximally entangled state to be of a particularly simple form, enabling us to express the exact positions of its MPs and CPPs analytically. In some cases, however, no analytical expressions were found for the positions of the CPPs and/or MPs. In these cases the exact amount of entanglement remains unknown, although it can be numerically approximated with high precision.

In this way we can be quite confident of finding the maximally entangled positive symmetric state. In the general symmetric case we do not have as many tools, so the search is over a far bigger set of possible states, and we

can be less confident in our results. We therefore focus our search to sets of states that promised high entanglement. Such states include those with highly spread out MP distributions, particularly the solutions of the classical optimization problems. From these results we can propose candidates for maximal symmetric entanglement.

For two and three qubits, the maximally entangled symmetric states are known and were discussed in Section IV, so we start with four qubits. A table summarizing the amount of entanglement of the numerically determined maximally entangled positive symmetric as well as the entanglement of the candidates for the general symmetric case can be found in Appendix C.

A. Four qubits

For four points, both Tóth's and Thomson's problem are solved by the vertices of the regular tetrahedron [66]. The numerical search for the maximally entangled symmetric state returns the Platonic solid too. Recast as MPs, the vertices are

$$\begin{aligned} |\phi_1\rangle &= |0\rangle, \\ |\phi_2\rangle &= \frac{1}{\sqrt{3}}|0\rangle + \sqrt{\frac{2}{3}}|1\rangle, \\ |\phi_3\rangle &= \frac{1}{\sqrt{3}}|0\rangle + e^{i2\pi/3}\sqrt{\frac{2}{3}}|1\rangle, \\ |\phi_4\rangle &= \frac{1}{\sqrt{3}}|0\rangle + e^{i4\pi/3}\sqrt{\frac{2}{3}}|1\rangle. \end{aligned} \quad (29)$$

The symmetric state constructed from these MPs by means of Equation (10) shall be referred to as the 'tetrahedron state'. Its form is $|\Psi_4\rangle = \sqrt{1/3}|S_0\rangle + \sqrt{2/3}|S_3\rangle$, and its MP distribution is shown in Figure 4. Because the state is positive and has a rotational symmetry around the Z-axis, Lemma 6 restricts the possible CPP locations to the three half-circles $|\sigma(\theta, \varphi)\rangle$ with $\varphi = 0, 2\pi/3, 4\pi/3$. From the symmetry of the Platonic solid it is clear that the MP distribution of Figure 4 can be rotated s.t. $|\phi_2\rangle$, $|\phi_3\rangle$ or $|\phi_4\rangle$ is moved to the north pole, with the actual distribution (and thus $|\Psi_4\rangle$) remaining unchanged. Each of these rotations, however, gives rise to new restrictions on the location of the CPPs mediated by Lemma 6. The intersections of all these restrictions are the four points where the MPs lie. This yields the result that $|\Psi_4\rangle$ has

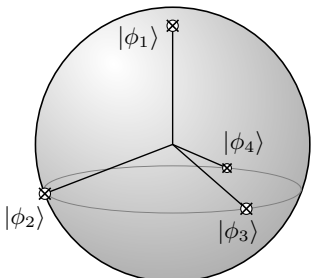


FIG. 4. MPs and CPPs of the 'tetrahedron state'.

four CPPs, with their Bloch vectors being the same as those in Equation (29). From this the amount of entanglement follows as $E_G(|\Psi_4\rangle) = \log_2 3 \approx 1.59$.

B. Five qubits

For five points, the solution to Thomson's problem is given by three of the charges lying on the vertices of an equatorial triangle and the other two lying at the poles [78, 86]. This is also a solution to Tóth's problem, but it is not unique [83, 87]. The corresponding quantum state, the 'trigonal bipyramid state', is shown in Figure 5(a). This state has the form $|\psi_5\rangle = 1/\sqrt{2}(|S_1\rangle + |S_4\rangle)$, and a simple calculation yields that it has three CPPs that coincide with the equatorial MPs, giving an entanglement of $E_G(|\psi_5\rangle) = \log_2(16/5) \approx 1.68$.

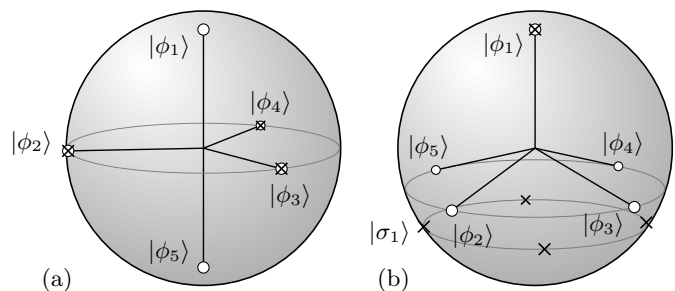


FIG. 5. The distribution (a) shows the 'trigonal bipyramid state', but the conjectured solution of the Majorana problem is the 'square pyramid state', shown in (b).

However, a numerical search among all positive symmetric states yields states with higher entanglement. Our numerics indicate that the maximally entangled state is the 'square pyramid state' shown in Figure 5(b). This state has five CPPs, one on the north pole and the other four lying in a horizontal plane slightly below the plane with the MPs. The form of this state is

$$|\Psi_5\rangle = \frac{1}{\sqrt{1+A^2}}|S_0\rangle + \frac{A}{\sqrt{1+A^2}}|S_4\rangle. \quad (30)$$

Its MPs are

$$\begin{aligned} |\phi_1\rangle &= |0\rangle, \\ |\phi_{2,3,4,5}\rangle &= \alpha|0\rangle + e^{i\kappa}\sqrt{1-\alpha^2}|1\rangle, \end{aligned} \quad (31)$$

with $\kappa = \frac{\pi}{4}, \frac{3\pi}{4}, \frac{5\pi}{4}, \frac{7\pi}{4}$, and the CPPs are

$$\begin{aligned} |\sigma_1\rangle &= |0\rangle, \\ |\sigma_{2,3,4,5}\rangle &= x|0\rangle + k\sqrt{1-x^2}|1\rangle, \end{aligned} \quad (32)$$

with $k = 1, i, -1, -i$. The exact values can be determined analytically by solving quartic equations. The $x \in (0, 1)$ of Equation (32) is given by the real root of $4x^4 + 4x^3 + 4x^2 - x - 1 = 0$, and this can be used to calculate $A = (1-x^5)/(\sqrt{5}x(1-x^2)^2)$. With the substitution $a = \alpha^2 \in (0, 1)$ the value of α is given by the real root of

$(5A^2 - 1)a^4 + 4a^3 - 6a^2 + 4a - 1 = 0$. Approximate values of these quantities are:

$$x \approx 0.46657, \quad A \approx 1.53154, \quad \alpha \approx 0.59229. \quad (33)$$

The entanglement is $E_G(|\Psi_5\rangle) = \log_2(1 + A^2) \approx 1.74$, which is considerably higher than that of $E_G(|\psi_5\rangle)$. We remark that the ‘center of mass’ of the five MPs of $|\Psi_5\rangle$ does not coincide with the sphere’s origin, thus ruling out the corresponding spin-5/2 state as an anticoherent spin state, as defined in [51].

C. Six qubits

The regular octahedron, a Platonic solid, is the unique solution to Tóth’s and Thomson’s problem for six points. The corresponding ‘octahedron state’ was numerically confirmed to solve the Majorana problem for six qubits.

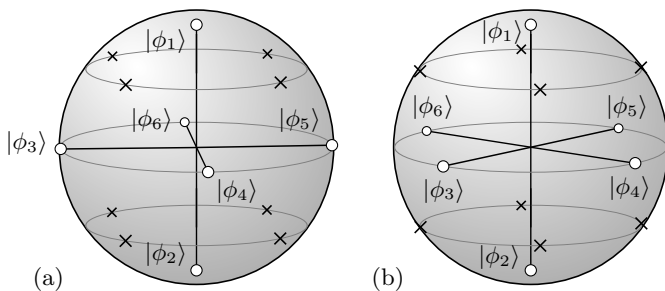


FIG. 6. Two possible orientations of the ‘octahedron state’.

The straightforward orientation shown in Figure 6(a) has the form $|\Psi'_6\rangle = 1/\sqrt{2}(|S_1\rangle - |S_5\rangle)$, and its MPs are

$$\begin{aligned} |\phi_1\rangle &= |0\rangle, \quad |\phi_2\rangle = |1\rangle, \\ |\phi_{3,4,5,6}\rangle &= \frac{1}{\sqrt{2}}(|0\rangle + k|1\rangle), \end{aligned} \quad (34)$$

with $k = 1, i, -1, -i$. $|\Psi'_6\rangle$ can be turned into the positive state $|\Psi_6\rangle = 1/\sqrt{2}(|S_1\rangle + |S_5\rangle)$ by means of an $R_z^s(\pi/4)$ rotation. The CPPs can be obtained from this state in the same way as for the tetrahedron state. Being a Platonic solid, the MP distribution of Figure 6(b) is left invariant under a finite subgroup of rotation operations on the sphere. From Lemma 6, the intersection of the permissible locations of the CPPs is found to be the eight points lying at the center of each face of the octahedron, forming a cube inside the Majorana sphere.

$$\begin{aligned} |\sigma_{1,2,3,4}\rangle &= \sqrt{\frac{\sqrt{3}+1}{2\sqrt{3}}} |0\rangle + k\sqrt{\frac{\sqrt{3}-1}{2\sqrt{3}}} |1\rangle, \\ |\sigma_{5,6,7,8}\rangle &= \sqrt{\frac{\sqrt{3}-1}{2\sqrt{3}}} |0\rangle + k\sqrt{\frac{\sqrt{3}+1}{2\sqrt{3}}} |1\rangle, \end{aligned} \quad (35)$$

with $k = 1, i, -1, -i$. In contrast to the tetrahedron state, where the MPs and CPPs overlap, the CPPs of the octahedron state lie as far away from the MPs as possible. This is plausible, because in the case of the octahedron Equation (20) is zero at the location of any MP, due to the MPs forming diametrically opposite pairs. The amount of entanglement is $E_G(|\Psi_6\rangle) = \log_2(9/2) \approx 2.17$.

D. Seven qubits

For seven points, the solutions to the two classical problems become fundamentally different for the first time. Tóth’s problem is solved by two triangles asymmetrically positioned about the equator and the remaining point at the north pole [76], or (1-3-3) in the Föppl notation [66]. Thomson’s problem is solved by the vertices of a pentagonal dipyrmaid [76, 78, 86], where five points lie on an equatorial pentagon and the other two on the poles. The latter is also numerically found to be the solution to the Majorana problem.

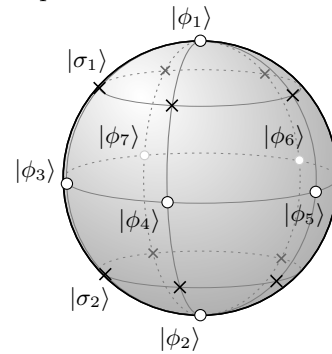


FIG. 7. MPs and CPPs of the ‘pentagonal dipyrmaid state’. The ten CPPs are equidistantly located on two circles above and below the equator.

The ‘pentagonal dipyrmaid state’, shown in Figure 7, has the form $|\Psi_7\rangle = 1/\sqrt{2}(|S_1\rangle + |S_6\rangle)$, and its MPs are

$$\begin{aligned} |\phi_1\rangle &= |0\rangle, \quad |\phi_2\rangle = |1\rangle, \\ |\phi_{3,4,5,6,7}\rangle &= \frac{1}{\sqrt{2}}(|0\rangle + e^{i\kappa}|1\rangle), \end{aligned} \quad (36)$$

with $\kappa = 0, \frac{2\pi}{5}, \frac{4\pi}{5}, \frac{6\pi}{5}, \frac{8\pi}{5}$. The CPPs of this positive state can be determined analytically by choosing a suitable parametrization. With $x := \cos^2\theta$ the position of $|\sigma_1\rangle = c_\theta|0\rangle + s_\theta|1\rangle$ and $|\sigma_2\rangle = s_\theta|0\rangle + c_\theta|1\rangle$ is determined by the real root of the cubic equation $49x^3 + 165x^2 - 205x + 55 = 0$ in the interval $[0, \frac{1}{2}]$. The approximate amount of entanglement is $E_G(|\Psi_7\rangle) \approx 2.299$.

E. Eight qubits

For eight points, Tóth’s problem is solved by the cubic antiprism, a cube with one face rotated around 45° and where the distances between neighboring vertices are all the same. The solution to Thomson’s problem is obtained by stretching this cubic antiprism along the Z-axis, thereby introducing two different nearest-neighbor distances and further lowering symmetry [76, 78, 86]. One would expect that a similar configuration solves the Majorana problem too, but, surprisingly, this is not the case. The ‘asymmetric pentagonal dipyrmaid’ shown in Figure 8(b) is numerically found to have the highest amount of entanglement. An analytic form of this positive state is not known, but it can be numerically approximated to a very

high precision. The state is $|\Psi_8\rangle \approx 0.672|S_1\rangle + 0.741|S_6\rangle$, and its entanglement is $E_G(|\Psi_8\rangle) \approx 2.45$. For comparison, the regular cube yields $E_G(|\psi_{\text{cube}}\rangle) = \log_2(24/5) \approx 2.26$. Interestingly, the positive state $|\Psi_8\rangle$ has a higher amount of entanglement than any state of the antiprism form, all of which are non-positive. Furthermore, two of the MPs of $|\Psi_8\rangle$ coincide, akin to the W state of three qubits.

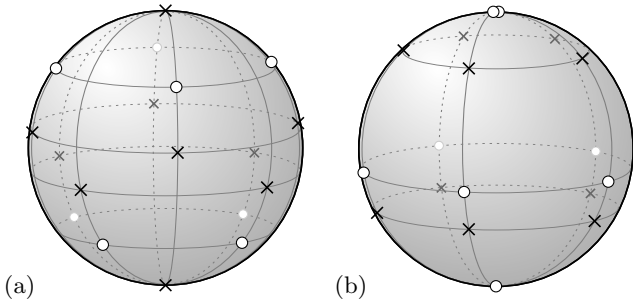


FIG. 8. The maximally entangled antiprism state is shown in (a), while the ‘asymmetric pentagonal dipyrmaid state’ in (b) is conjectured to be the maximally entangled state.

$|\Psi_8\rangle$ is positive, with two MPs lying on the north pole, one on the south pole and the other five on a circle below the equator. The exact inclination of this circle as well as the inclination of the two circles with the CPPs is not known, but can be approximated numerically.

F. Nine qubits

For nine points, the solutions to Tóth’s and Thomson’s problems are slightly different manifestations of the same geometric form (3-3-3) of neighboring triangles being asymmetrically positioned. This is also known as a triaugmented triangular prism. In contrast to this, the Majorana problem is numerically solved by $|\Psi_9\rangle = 1/\sqrt{2}(|S_2\rangle + |S_7\rangle)$, shown in Figure 9. This is again a positive state with a rotational Z-axis symmetry and with coinciding MPs.

The CPPs can be found analytically in the same way as for seven qubits. With the substitution $x := \cos^2 \theta$, the

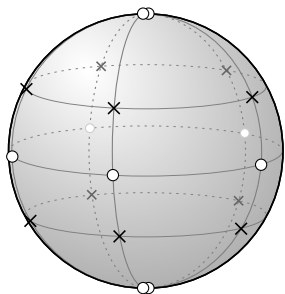


FIG. 9. The ‘pentagonal dipyrmaid state’ with both of the poles occupied by two MPs.

inclination θ of the CPPs in the northern hemisphere (or $\pi - \theta$ for the CPPs in the southern hemisphere) follows from the real root of $81x^3 + 385x^2 - 245x + 35 = 0$ in the interval $[0, 0.3]$. The approximate amount of entanglement is $E_G(|\Psi_9\rangle) \approx 2.554$.

G. Ten qubits

The solution to Tóth’s problem is an arrangement of the form (2-2-4-2), while Thomson’s problem is solved by the gyroelongated square bipyramid, a deltahedron that arises from a cubic antiprism by placing square pyramids on each of the two square surfaces.

The ten-qubit case is distinct in two respects. It is the first case where the numerically determined positive solution is not rotationally symmetric around any axis. Furthermore, we found non-positive states with higher entanglement than the conjectured solution for positive states.

A numerical search returns a state of the form $|\Psi_{10}\rangle = \alpha|S_0\rangle + \beta|S_4\rangle + \gamma|S_9\rangle$ as the positive state with the highest entanglement, namely $E_G(|\Psi_{10}\rangle) \approx 2.6798$. From Lemma 3 it is clear that this state is not rotationally symmetric around the Z-axis. The MP distribution is shown in Figure 10(a). The state has only three CPPs, which are all positive (cf. Theorem 1), but there are six other local maxima of $g(\sigma)$ with values close to the CPPs. Their positions are shown by dashed crosses in Figure 10(a). While the total MP distribution is not rotationally symmetric around the Z-axis, one would expect from the numerical results that the MPs form two horizontal planes, one with five MPs and another with four MPs, with equidistantly spread out MPs. However, this is not the case, as the locations of the MPs deviate by small, but significant, amounts from this simple form.

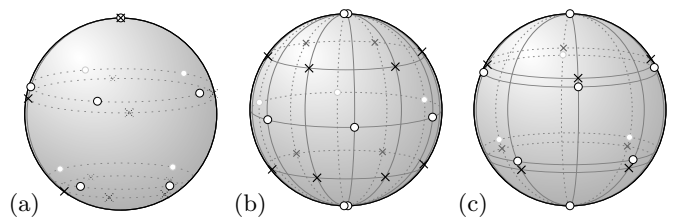


FIG. 10. The numerically determined maximally entangled positive state is shown in (a). A similarly highly entangled positive state with a rotational symmetry is shown in (b). The candidate for the general case is shown in (c).

Interestingly, there is a fully rotationally symmetric positive state that comes very close to $|\Psi_{10}\rangle$ in terms of entanglement. Its straightforward form is $|\psi_{10}\rangle = 1/\sqrt{2}(|S_2\rangle + |S_8\rangle)$, as displayed in Figure 10(b). The 12 CPPs of this state are easily found as the solutions of a

quadratic equation. The two positive CPPs are

$$\begin{aligned} |\sigma_1\rangle &= \frac{1}{\sqrt{3-\sqrt{3}}} |0\rangle + \frac{1}{\sqrt{3+\sqrt{3}}} |1\rangle, \\ |\sigma_2\rangle &= \frac{1}{\sqrt{3+\sqrt{3}}} |0\rangle + \frac{1}{\sqrt{3-\sqrt{3}}} |1\rangle, \end{aligned} \quad (37)$$

and the entanglement is $E_G(|\psi_{10}\rangle) = \log_2(32/5) \approx 2.6781$. This is less than 0.1% difference from $|\Psi_{10}\rangle$.

The solution to Thomson's problem, recast as a quantum state of the form $|\Psi'_{10}\rangle = \alpha|S_1\rangle + \beta|S_5\rangle - \alpha|S_9\rangle$, is not positive and has an entanglement of $E_G \approx 2.7316$. From numerics one can see that the entanglement of this state can be further increased by slightly modifying the coefficients, arriving at a state with eight CPPs and an entanglement of $E_G(|\Psi'_{10}\rangle) \approx 2.7374$. The state is shown in Figure 10(c), and we propose it as a candidate for the maximally entangled symmetric state of ten qubits.

H. Eleven qubits

The solution to Tóth's problem is a pentagonal antiprism with a pentagonal pyramid on one of the two pentagonal surfaces, or (1-5-5). The solution to Thomson's problem is of the form (1-2-4-2-2). Analogous to the ten-qubit case, the numerically found positive state of 11 qubits with maximal entanglement is not rotationally symmetric. The state, shown in Figure 11(a), is of the form $|\Psi_{11}\rangle = \alpha|S_1\rangle + \beta|S_5\rangle + \gamma|S_{10}\rangle$, and its entanglement is $E_G(|\Psi_{11}\rangle) \approx 2.77$. The state has only two CPPs, but there exist seven more local maxima with values close to the CPPs.

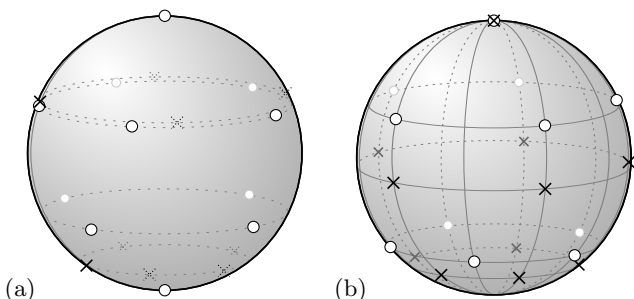


FIG. 11. The conjectured maximally entangled positive state of 11 qubits is shown in (a), while the candidate for the general case is shown in (b).

The solution to Tóth's problem, which is of the form $|\psi'_{11}\rangle = \alpha|S_0\rangle + \beta|S_5\rangle - \gamma|S_{10}\rangle$, yields very low entanglement, but by modifying the coefficients of this non-positive state one can find a state $|\Psi'_{11}\rangle$ which is even more entangled than $|\Psi_{11}\rangle$. As shown in Figure 11(b), the state is rotationally symmetric around the Z-axis and has 11 CPPs. The entanglement is $E_G(|\Psi'_{11}\rangle) \approx 2.83$, making the state the potentially maximally entangled state of 11 qubits.

I. Twelve qubits

For 12 points, both of the classical problems are solved by the icosahedron, a Platonic solid. Because the icosahedron cannot be cast as a positive state, the numerical search for positive states yields a different state of the form $|\Psi'_{12}\rangle = \alpha|S_1\rangle + \beta|S_6\rangle + \alpha|S_{11}\rangle$. From Figure 12(a) it can be seen that this state can be thought of as an icosahedron with one circle of MPs rotated by 36° so that it is aligned with the MPs of the other circle. There are three circles of CPPs with five in each circle. One of these planes coincides with the equator, so that $|\sigma\rangle = 1/\sqrt{2}(|0\rangle + |1\rangle)$ is a trivial CPP. Nevertheless, the exact location of some of the MPs and CPPs are unknown. The approximate entanglement is $E_G(|\Psi'_{12}\rangle) \approx 2.99$.

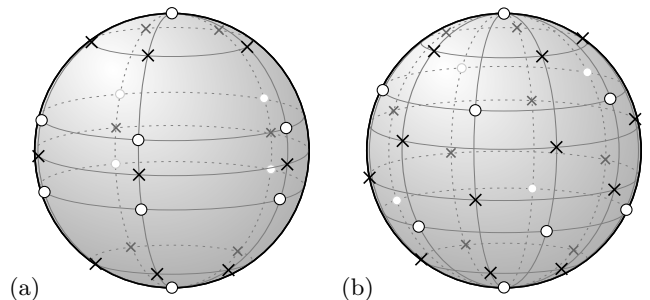


FIG. 12. An orientation of the maximally entangled positive symmetric state of 12 qubits is shown in (a). The icosahedron state, shown in (b), is considered to be the maximally entangled of all symmetric 12 qubit states.

Due to the high symmetry present in Platonic solids, the 'icosahedron state' is a strong candidate for maximal symmetric entanglement of twelve qubit states. The state can be cast with real coefficients $|\Psi_{12}\rangle = \frac{\sqrt{7}}{5}|S_1\rangle - \frac{\sqrt{11}}{5}|S_6\rangle - \frac{\sqrt{7}}{5}|S_{11}\rangle$, and its MPs can be easily derived from the known angles and distances in the icosahedron.

$$\begin{aligned} |\phi_1\rangle &= |0\rangle, \quad |\phi_{12}\rangle = |1\rangle, \\ |\phi_{2,3,4,5,6}\rangle &= \sqrt{\frac{3+\sqrt{5}}{5+\sqrt{5}}} |0\rangle + e^{i\kappa} \sqrt{\frac{2}{5+\sqrt{5}}} |1\rangle, \\ |\phi_{7,8,9,10,11}\rangle &= \sqrt{\frac{2}{5+\sqrt{5}}} |0\rangle + e^{i(\kappa+\pi/5)} \sqrt{\frac{3+\sqrt{5}}{5+\sqrt{5}}} |1\rangle, \end{aligned} \quad (38)$$

with $\kappa = 0, \frac{2\pi}{5}, \frac{4\pi}{5}, \frac{6\pi}{5}, \frac{8\pi}{5}$. From numerics and from the Z-axis rotational symmetry, it is evident that there are 20 CPPs, one at the center of each face of the icosahedron. Equivalent to the six-qubit case, the MPs appear as diametrically opposite pairs, forcing the CPPs to be as remote from the MPs as possible. The CPPs are

$$\begin{aligned} |\sigma_{1,\dots,5}\rangle &= a_+|0\rangle + e^{i(\kappa+\pi/5)} a_-|1\rangle, \\ |\sigma_{6,\dots,10}\rangle &= b_+|0\rangle + e^{i(\kappa+\pi/5)} b_-|1\rangle, \\ |\sigma_{11,\dots,15}\rangle &= b_-|0\rangle + e^{i\kappa} b_+|1\rangle, \\ |\sigma_{16,\dots,20}\rangle &= a_-|0\rangle + e^{i\kappa} a_+|1\rangle, \end{aligned} \quad (39)$$

with $\kappa = 0, \frac{2\pi}{5}, \frac{4\pi}{5}, \frac{6\pi}{5}, \frac{8\pi}{5}$ and

$$\begin{aligned} a_{\pm} &= \sqrt{\frac{1}{2} \pm \frac{1}{2} \sqrt{\frac{5+2\sqrt{5}}{15}}}, \\ b_{\pm} &= \sqrt{\frac{1}{2} \pm \frac{1}{2} \sqrt{\frac{5-2\sqrt{5}}{15}}}. \end{aligned} \quad (40)$$

With the knowledge of the exact positions of the MPs and CPPs, the entanglement of the icosahedron state can be calculated as $E_G(|\Psi_{12}\rangle) = \log_2(243/28) \approx 3.1175$. Figure 13 shows a spherical plot of the overlap function $g(\sigma) = |\langle \Psi_{12} | \sigma \rangle^{\otimes 12}|$ from the same viewpoint as in Figure 12(b). Due to their diametrically opposite pairs, the MPs coincide with the zeros in this plot. The CPPs can be identified as the maxima of $g(\sigma)$.

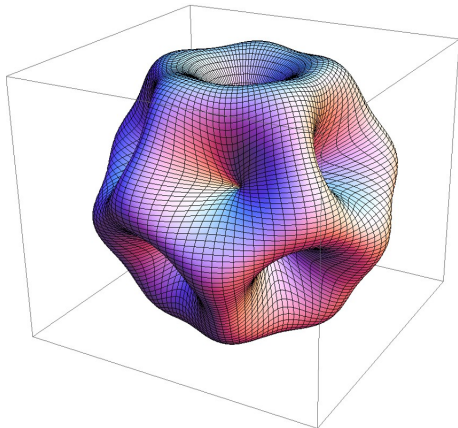


FIG. 13. (color online) A spherical plot of the overlap function $g(\sigma) = |\langle \Psi_{12} | \sigma \rangle^{\otimes 12}|$ for the icosahedron state $|\Psi_{12}\rangle$.

VII. DISCUSSION

The MP distribution of highly entangled states can be explained with the overlap function $g(\sigma) = |\langle \psi | \sigma \rangle^{\otimes n}|$ seen in Figure 13. Appendix A states that the integration volume of $g(\sigma)^2$ over the sphere is the same for all symmetric states. Therefore a bunching of the MPs in a small area of the sphere would lead to high values of $g(\sigma)^2$ in that area, thus lowering the entanglement. This explains the tendency of MPs to spread out as far as possible, as it is seen for the classical problems. However, there also exist highly entangled states where two or more MPs coincide (as seen for $n = 3, 8, 9$). This is intriguing because such configurations are the least optimal ones for classical problems. Again, this can be explained with the constant integration volume of $g(\sigma)^2$. Because of $g(\sigma)^2 \propto \prod_i |\langle \phi_i | \sigma \rangle|^2$, the zeros of $g(\sigma)^2$ are the diametrically opposite points (antipodes) of the MPs and therefore a lower number of *different* MPs leads to a lower number of zeros in $g(\sigma)^2$. This can lead to the

integration volume being more evenly distributed over the sphere, thus yielding a higher amount of entanglement.

Excluding the Dicke states with their infinite amount of CPPs, one observes that highly entangled states tend to have a large number of CPPs. The prime example for this is the case of five qubits, where the classical solution with only three CPPs is less entangled than the ‘square pyramid’ state that has five CPPs. In Theorem 1 it was shown that $2n - 4$ is an upper bound on the number of CPPs of positive symmetric n qubit states. For all of our numerically determined maximally entangled states – including the non-positive ones – this bound is obeyed, and for most states the number of CPPs is close to the bound ($n = 5, 8$) or coincides with it ($n = 4, 6, 7, 12$). This raises the question whether this bound also holds for general symmetric states. To date, neither proof nor counterexample is known.

When viewing the n MPs of a symmetric state as the edges of a polyhedron, Euler’s formula for convex polyhedra yields the upper bound $2n - 4$ on the number of faces. This bound is strict if no pair of MPs coincides and all polyhedral faces are triangles. Intriguingly, this bound is the same as the one for CPPs mentioned in the previous paragraph, and the polyhedral faces of our numerical solutions come close to the bound ($n = 5, 8, 11$) or coincide with it ($n = 4, 6, 7, 10, 12$). The faces of the polyhedron associated with the Majorana representation might therefore hold the key to a proof for $2n - 4$ being the upper bound on the number of CPPs for all symmetric states (with only the Dicke states excluded).

The case of ten qubits seems to be the first one where the maximally entangled symmetric state cannot be cast as a positive state. For $n = 10, 11, 12$, our candidates for maximal entanglement are real states, so the question remains whether the maximally entangled state can always be cast with real coefficients. We consider this unlikely, firstly because of the higher amount of MP freedom in the general case and secondly because many of the solutions to the classical problems cannot be cast as real MP distributions for higher n . For Thomson’s problem, the first distribution without any symmetry (and thus no representation as a real state) arises at $n = 13$, and for Tóth’s problem at $n = 15$.

Upper and lower bounds on the maximal entanglement of symmetric states have already been discussed in Section III, with a new proof for the upper bound given in Appendix A. Stronger lower bounds can be computed from the known solutions to Tóth’s and Thomson’s problems by translating their point distribution into the corresponding symmetric state and determining its entanglement. The diagram in Figure 14 displays the entanglement of our numerical solutions, together with all bounds.

For $n > 5$ qubits, the maximally entangled state cannot be symmetric or turned into one by LOCC, because the lower bound on general states is higher than the upper bound of symmetric states. For $n = 3$, the maximally entangled state (W state) is demonstrably symmetric, but for $n = 4, 5$ the numerical solutions for symmetric states have less entanglement than the lower bound of

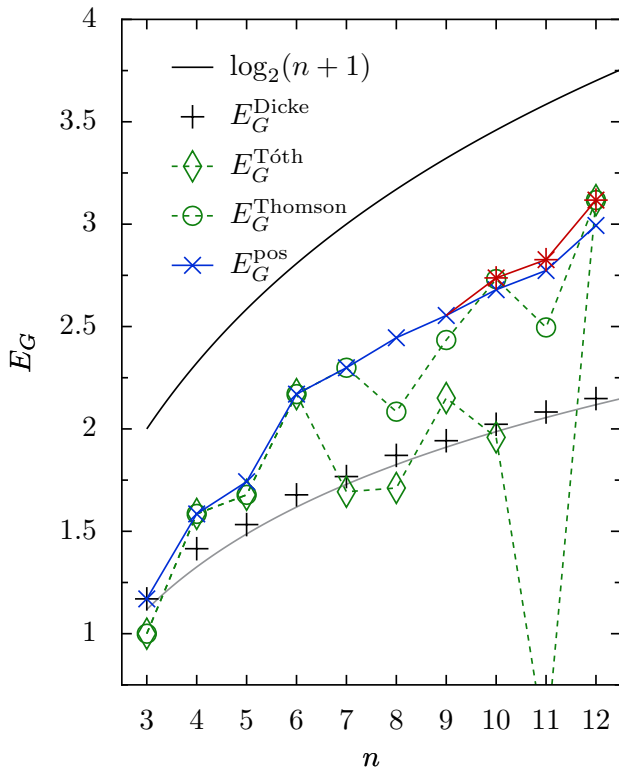


FIG. 14. (color online) Scaling of maximal symmetric entanglement with the number of qubits n . The upper bound is represented by a black line, while the most entangled Dicke states form the lower bound. Their Stirling approximation is displayed as a grey line. The most entangled positive symmetric states found are denoted by blue crosses. For $n = 10 - 12$, the best candidates cannot be cast with positive coefficients and are depicted as red stars. The solutions of Tóth’s and Thomson’s problems readily provide lower bounds, displayed as dashed green lines. The solutions of Thomson’s problem are generally more highly entangled than those of Tóth’s problem.

general states. This would imply that n qubit maximally entangled states can be symmetric if, and only if, $n \leq 3$.

VIII. CONCLUSION

In this paper, we have investigated the maximally entangled state among symmetric quantum states of n qubits. By visualizing symmetric states through the Majorana representation and with the help of analytical and numerical methods, strong candidates for the maximally entangled symmetric states of up to 12 qubits were found. A comparison with the extremal distributions of Tóth’s and Thomson’s problems shows that, in some cases, the optimal solution to Majorana’s problem coincides with that of the two classical problems, but in other cases it significantly differs.

Lower and upper bounds show that the maximal entanglement of permutation-symmetric qubit states scales between $\mathcal{O}(\log \sqrt{n})$ and $\mathcal{O}(\log n)$ with the number of qubits

n . With respect to MBQC, these results indicate that, although permutation-symmetric states may not be good resources for deterministic MBQC, they may be good for stochastic approximate MBQC [8, 9]. It also gives bounds on how much information can be discriminated locally, for which explicit protocols are known in some cases (in particular for Dicke states) [5, 10].

We remark that, due to the close relationship of distance-like entanglement measures [5], the results for the geometric measure give bounds to the robustness of entanglement and the relative entropy of entanglement, which can be shown to be tight in certain cases of high symmetry [10, 23].

We finally note that a similar study has been carried out, although from a different perspective, in search of the ‘least classical’ state of a single spin- j system [52] (which they call the ‘queens of quantumness’). There the Majorana representation is used to display spin- j states, through the well-known isomorphism between a single spin- j system and the symmetric state of $n = 2j$ spin- $1/2$ systems. In this context, the most ‘classical’ state is the spin coherent state, which corresponds exactly to a symmetric product state in our case (i.e. n coinciding MPs). The problem of [52] is similar to ours in that they look for the state ‘furthest away’ from the set of spin coherent states. However, different distance functions are used, so the optimization problem is subtly different and again yields different solutions. It is in any case interesting to note that our results also have interpretations in this context and vice versa.

ACKNOWLEDGMENTS

The authors thank S. Miyashita, S. Virmani, A. Soeda and K.-H. Borgwardt for very helpful discussions. This work was supported by the National Research Foundation & Ministry of Education, Singapore, and the project ‘Quantum Computation: Theory and Feasibility’ in the framework of the CNRS-JST Strategic French-Japanese Cooperative Program on ICT. MM thanks the ‘Special Co-ordination Funds for Promoting Science and Technology’ for financial support.

Note added. During the completion of this manuscript, we became aware of very similar work that also looks at the maximum entanglement of permutation-symmetric states using very similar techniques [88].

Appendix A: Upper bound on symmetric entanglement

A symmetric n qubit state can be written as

$$|\psi\rangle = \sum_{k=0}^n a_k e^{i\alpha_k} |S_k\rangle, \quad (A.1)$$

with $a_k \in \mathbb{R}$, $\alpha_k \in [0, 2\pi)$ and the normalization condition $\sum_k a_k^2 = 1$. Writing the closest product state as $|\lambda\rangle =$

$|\sigma\rangle^{\otimes n}$ with $|\sigma\rangle = c_\theta|0\rangle + e^{i\varphi}s_\theta|1\rangle$, we obtain

$$\langle\lambda|\psi\rangle = \sum_{k=0}^n e^{i(\alpha_k - k\varphi)} a_k c_\theta^{n-k} s_\theta^k \sqrt{\binom{n}{k}}. \quad (\text{A1})$$

Using the set of qubit unit vectors \mathcal{H}_1 and the uniform measure over the unit sphere $d\mathcal{B}$, the squared norm of Equation (A1) can be integrated over the Majorana sphere:

$$\int_{|\sigma\rangle \in \mathcal{H}_1} |\langle\lambda|\psi\rangle|^2 d\mathcal{B} = \int_0^{2\pi} \int_0^\pi |\langle\lambda|\psi\rangle|^2 \sin\theta d\theta d\varphi. \quad (\text{A2})$$

Taking into account that $\int_0^{2\pi} e^{im\varphi} d\varphi = 0$ for any integer $m \neq 0$, one obtains

$$\int_0^{2\pi} \int_0^\pi \left[\sum_{k=0}^n a_k^2 c_\theta^{2(n-k)} s_\theta^{2k} \binom{n}{k} \right] \sin\theta d\theta d\varphi, \quad (\text{A3a})$$

$$= 2\pi \sum_{k=0}^n a_k^2 \binom{n}{k} \int_0^\pi c_\theta^{2(n-k)} s_\theta^{2k} \sin\theta d\theta, \quad (\text{A3b})$$

$$= 4\pi \sum_{k=0}^n a_k^2 \binom{n}{k} \frac{\Gamma(k+1)\Gamma(n-k+1)}{\Gamma(n+2)}, \quad (\text{A3c})$$

$$= 4\pi \sum_{k=0}^n a_k^2 \frac{1}{n+1} = \frac{4\pi}{n+1}. \quad (\text{A3d})$$

The equivalence of Equations (A3b) and (A3c) follows from the different definitions of the Beta function [89]. Since the mean value of $|\langle\lambda|\psi\rangle|^2$ over the Majorana sphere is $4\pi/(n+1)$, it follows that $G(|\psi\rangle)^2 \geq 1/(n+1)$, or $E_G(|\psi\rangle) \leq \log_2(n+1)$, for any symmetric n qubit state.

This result was first shown by R. Renner in his PhD thesis [46], using a similar proof that employs an explicit separable decomposition of the identity over symmetric subspace. The same proof as ours was independently found by J. Martin *et al.* [88].

Appendix B: Proof of theorem 1

Class (b): We consider states that have a Z-axis rotational symmetry with minimal rotational angle $\varphi = 2\pi/m$, $m \in \mathbb{N}$ and $1 < m \leq n$. Figure 15 shows an example for $m = 5$. Due to the rotational Z-axis symmetry and the reflective symmetry imposed by Theorem 5, the MPs are restricted to specific distribution patterns. An arbitrary number of MPs can lie on each of the poles, with the remaining MPs equidistantly aligned along horizontal circles. The figure shows the two principal types of horizontal circles that can exist. The upper one is the basic type for positive states of five qubits, and the lower one a special case where two basic circles are intertwined at azimuthal angle $\pm\vartheta$ from the position of the single basic circle, respectively. All conceivable horizontal circles of MPs can be decomposed into these two principal types.

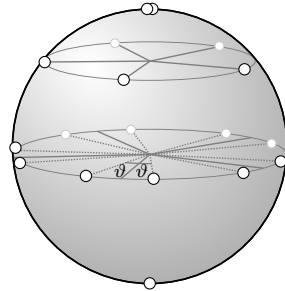


FIG. 15. An example of a positive state of 18 qubits with a rotational symmetry around the Z-axis with angle $\varphi = 2\pi/5$. Two MPs lie on the north pole, one on the south pole, five on a single basic circle and ten on two intertwined basic circles.

According to Equation (14), any CPP $|\sigma\rangle$ maximizes the function $\prod_{i=1}^n |\langle\sigma|\phi_i\rangle|$, where the $|\phi_i\rangle$ are the MPs. From Lemma 1 it follows that there must be at least one positive $|\sigma\rangle = c_\theta|0\rangle + s_\theta|1\rangle$. We first derive the maximum number of positive CPPs, and from these the upper bound for the total number of CPPs can be immediately obtained with the help of Lemma 6.

For a MP distribution with k MPs on the north pole, l MPs on the south pole and the remaining $n - k - l$ MPs on horizontal circles, the function to maximize is

$$f(\theta) = \langle\sigma|0\rangle^k \langle\sigma|1\rangle^l \prod_r h_1(\theta_r) \prod_s h_2(\vartheta_s, \theta_s),$$

where $h_1(\theta_r)$ represents the factors contributed by a single basic circle with m MPs at inclination θ_r , and $h_2(\vartheta_s, \theta_s)$ represents the factors contributed by two basic circles with $2m$ MPs intertwined at azimuthal angles $\pm\vartheta_s$, and inclination θ_s . It is easy to verify that

$$h_1(\theta_r) = c_\theta^m c_{\theta_r}^m + s_\theta^m s_{\theta_r}^m, \\ h_2(\vartheta_s, \theta_s) = c_\theta^{2m} c_{\theta_s}^{2m} + 2 \cos(m\vartheta_s) c_\theta^m s_\theta^m c_{\theta_s}^m s_{\theta_s}^m + s_\theta^{2m} s_{\theta_s}^{2m}.$$

From this it is clear that f can be written in the form

$$f(\theta) = c_\theta^k s_\theta^l \sum_{i=0}^p a_i c_\theta^{(p-i)m} s_\theta^{im} = \sum_{i=0}^p a_i c_\theta^{k+(p-i)m} s_\theta^{l+im},$$

where the a_i are positive-valued coefficients, and p is the number of basic circles ($k + l + pm = n$). The number of zeros of $f'(\theta)$ in $\theta \in (0, \pi)$ gives a bound on the number of positive CPPs. The form of $f'(\theta)$ is qualitatively different for $m = 2$ and $m > 2$. With the substitution $x = \tan(\theta/2)$ the equation $f'(\theta) = 0$ for $m = 2$ becomes

$$a_0 l + \left(\sum_{i=1}^p b_i x^{2i} \right) - a_p k x^{2p+2} = 0, \quad \text{with} \\ b_i = a_i(l + 2i) - a_{i-1}(k + 2(p - i) + 2) \in \mathbb{R}.$$

This is a real polynomial in x , with the first and last coefficient vanishing if no MPs exist on the south pole ($l = 0$) and north pole ($k = 0$), respectively. Descartes'

rule of signs states that the number of positive roots of a real polynomial is at most the number of sign differences between consecutive nonzero coefficients, ordered by descending variable exponent. From this and the fact that the codomain of x is \mathbb{R}^+ , we obtain the result that for $m = 2$ there are at most $p - 1$, p or $p + 1$ extrema of $f(\theta)$ lying in $\theta \in (0, \pi)$, depending on whether k and l are zero or not.

For $m > 2$, we obtain the analogous result

$$a_0 l + \left(\sum_{i=1}^p -c_i x^{im-(m-2)} + d_i x^{im} \right) - a_p k x^{pm+2} = 0 ,$$

with $c_i = a_{i-1}(k + (p-i)m + m) \in \mathbb{R}^+$,
and $d_i = a_i(l + im) \in \mathbb{R}^+$.

From Descartes' rule of signs, we find that there exist $2p-1$, $2p$ or $2p+1$ extrema of $f(\theta)$ in $\theta \in (0, \pi)$, depending on whether k and l are zero or not.

With these results it is easy to determine the maximum number of global maxima of $f(\theta)$, which are the positive CPPs. Case differentiations have to be done with regard to $m = 2$ or $m > 2$, whether k and l are zero or not and whether p is even or odd. Due to the rotational Z-axis symmetry, the non-positive CPPs can be immediately obtained. For any positive CPP not lying on a pole, there are $m - 1$ other, non-positive CPPs lying at the same inclination (cf. Lemma 6). For $m = 2$, the maximum possible number of CPPs is $(n/2)+1$ (n even) or $(n+1)/2$ (n odd). This is significantly less than that in the general case $m > 2$, where the maximum number of CPPs is $2n - 4$. Interestingly, this bound decreases to n if at least one of the two poles is free of MPs.

Class (c): All MPs of a positive state must either lie on the positive meridian or form complex conjugate pairs (cf. Lemma 5). From this the optimization function is easily derived as

$$f(\theta) = \sum_{i=0}^n a_i c_\theta^{n-i} s_\theta^i ,$$

with real a_i . Calculating $f'(\theta)$ yields the condition for the extrema:

$$a_1 + \left(\sum_{i=1}^{n-1} b_i x^i \right) - a_{n-1} x^n = 0 ,$$

with $b_i = a_{i+1}(i+1) - a_{i-1}(n-i+1)$.

From this, the maximum number of CPPs can be derived with Descartes' rule. All CPPs are now restricted to the positive meridian and the poles, yielding at most $(n+3)/2$ CPPs for odd n and $(n+2)/2$ for even n . \square

Appendix C: Table of entanglement values

TABLE I. The table lists the known ($n = 2, 3$) and numerically determined ($n > 3$) values of the maximal entanglement of symmetric n qubit states. The left column lists the extremal entanglement among positive symmetric states, and, where more entangled non-positive symmetric states are known, they are displayed in the right column.

n	E_G^{pos}	E_G
2	1	
3	$2 \log_2 3 - 2 \approx 1.170$	
4	$\log_2 3 \approx 1.585$	
5	$\approx 1.742\ 268\ 948^a$	
6	$2 \log_2 3 - 1 \approx 2.170$	
7	$\approx 2.298\ 691\ 396^a$	
8	$\approx 2.445\ 210\ 159$	
9	$\approx 2.553\ 960\ 277^a$	
10	$\approx 2.679\ 763\ 092$	$\approx 2.737\ 432\ 003$
11	$\approx 2.773\ 622\ 669$	$\approx 2.817\ 698\ 505$
12	$\approx 2.993\ 524\ 700$	$\log_2(243/28) \approx 3.117$

^a The analytic form is known, but is of a complicated form.

-
- [1] R. Horodecki, P. Horodecki, M. Horodecki, and K. Horodecki, Rev. Mod. Phys. **81**, 865 (2009).
[2] W. Dür, G. Vidal, and J. I. Cirac, Phys. Rev. A **62**, 062314 (2000).
[3] A. Shimony, Ann. NY. Acad. Sci. **755**, 675 (1995).
[4] T.-C. Wei, M. Ericsson, P. M. Goldbart, and W. J. Munro, Quant. Inf. Comp. **4**, 252 (2004).
[5] M. Hayashi, D. Markham, M. Muraio, M. Owari, and S. Virmani, Phys. Rev. Lett. **96**, 040501 (2006).
[6] R. F. Werner and A. S. Holevo, J. Math. Phys. **43**, 4353 (2002).
[7] D. Gross, S. T. Flammia, and J. Eisert, Phys. Rev. Lett. **102**, 190501 (2009).
[8] M. Van den Nest, W. Dür, A. Miyake, and H. J. Briegel, New J. Phys. **9**, 204 (2007).
[9] C. E. Mora *et al.*, Phys. Rev. A **81**, 042315 (2010).
[10] M. Hayashi, D. Markham, M. Muraio, M. Owari, and S. Virmani, Phys. Rev. A **77**, 012104 (2008).
[11] D. Cavalcanti, Phys. Rev. A **73**, 044302 (2006).
[12] L. De Lathauwer, B. De Moor, and J. Vandewalle, SIAM J. Matrix Anal. Appl. **21**, 1324 (2000).
[13] T. Zhang and G. H. Golub, SIAM J. Matrix Anal. Appl. **23**, 534 (2001).
[14] E. Kofidis and P. A. Regalia, SIAM J. Matrix Anal. Appl. **23**, 863 (2002).
[15] H. Wang and N. Ahuja, IEEE Int. Conf. on Pattern Recognition, ICPR (Cambridge, UK) pp 44-47 (2004).
[16] G. Ni and Y. Wang, Math. Comput. Modelling **46**, 1345 (2007).
[17] V. De Silva and L. H. Lim, SIAM J. Matrix Anal. Appl. **30**, 1084 (2008).
[18] E. D'Hondt and P. Panangaden, Quant. Inf. Comp. **6**, 173 (2006).
[19] D. M. Greenberger, M. A. Horne, A. Shimony, and

- A. Zeilinger, *Am. J. Phys.* **58**, 1131 (1990).
- [20] R. H. Dicke, *Phys. Rev.* **93**, 99 (1954).
- [21] R. Prevedel *et al.*, *Phys. Rev. Lett.* **103**, 020503 (2009).
- [22] W. Wieczorek *et al.*, *Phys. Rev. Lett.* **103**, 020504 (2009).
- [23] D. Markham, arXiv:1001.0343 (2010).
- [24] G. Tóth and O. Gühne, *Phys. Rev. Lett.* **102**, 170503 (2009).
- [25] R. Hübener, M. Kleinmann, T.-C. Wei, C. González-Guillén, and O. Gühne, *Phys. Rev. A* **80**, 032324 (2009).
- [26] T. Bastin *et al.*, *Phys. Rev. Lett.* **103**, 070503 (2009).
- [27] P. Mathonet *et al.*, *Phys. Rev. A* **81**, 052315 (2010).
- [28] E. Majorana, *Nuovo Cimento* **9**, 43 (1932).
- [29] V. Vedral and M. B. Plenio, *Phys. Rev. A* **57**, 1619 (1998).
- [30] T.-C. Wei and P. M. Goldbart, *Phys. Rev. A* **68**, 042307 (2003).
- [31] H. Barnum and N. Linden, *J. Phys. A: Math. Gen.* **34**, 6787 (2001).
- [32] D. C. Brody and L. P. Hughston, *J. Geom. Phys.* **38**, 19 (2001).
- [33] R. F. Werner and M. M. Wolf, *Phys. Rev. A* **64**, 032112 (2001).
- [34] G. Vidal and R. Tarrach, *Phys. Rev. A* **59**, 141 (1999).
- [35] D. Markham, A. Miyake, and S. Virmani, *New J. Phys.* **9**, 194 (2007).
- [36] E. Jung *et al.*, *Phys. Rev. A* **77**, 062317 (2008).
- [37] H. Zhu, L. Chen, and M. Hayashi, *New J. Phys.* **12**, 083002 (2010).
- [38] M. B. Plenio and S. Virmani, *Quant. Inf. Comp.* **7**, 1 (2007).
- [39] G. Tóth, *J. Opt. Soc. Am. B* **24**, 275 (2007).
- [40] R. Orús, S. Dusuel, and J. Vidal, *Phys. Rev. Lett.* **101**, 025701 (2008).
- [41] J. K. Korbicz, J. I. Cirac, and M. Lewenstein, *Phys. Rev. Lett.* **95**, 120502 (2005).
- [42] J. K. Korbicz *et al.*, *Phys. Rev. A* **74**, 052319 (2006).
- [43] J. K. Stockton, J. M. Geremia, A. C. Doherty, and H. Mabuchi, *Phys. Rev. A* **67**, 022112 (2003).
- [44] M. Hayashi, D. Markham, M. Murao, M. Owari, and S. Virmani, *J. Math. Phys.* **50**, 122104 (2009).
- [45] T.-C. Wei and S. Severini, *J. Math. Phys.* **51**, 092203 (2010).
- [46] R. Renner, ETH Zurich, PhD Thesis, arXiv:quant-ph/0512258 (2005).
- [47] A trivial example of an n qubit state with $E_G = (n/2)$ are $(n/2)$ bipartite Bell states, each of which contributes 1 ebit. Another example is the 2D cluster state of n qubits, which has $E_G = (n/2)$ [35].
- [48] H. Bacry, *J. Math. Phys.* **15**, 1686 (1974).
- [49] J. Zimba and R. Penrose, *Stud. Hist. Phil. Sci.* **24**, 697 (1993).
- [50] R. Penrose and W. Rindler, *Spinors and Space-Time. Vol.1: Two-Spinor Calculus and Relativistic Fields* (Cambridge University Press, Cambridge, 1984).
- [51] J. Zimba, *Electron. J. Theor. Phys.* **3**, 143 (2006).
- [52] O. Giraud, P. A. Braun, and D. Braun, *New J. Phys.* **12**, 063005 (2010).
- [53] D. Markham and V. Vedral, *Phys. Rev. A* **67**, 042113 (2003).
- [54] J. H. Hannay, *J. Phys. A: Math. Gen.* **29**, L101 (1996).
- [55] J. H. Hannay, *J. Phys. A: Math. Gen.* **31**, L53 (1998).
- [56] P. Leboeuf, *J. Phys. A: Math. Gen.* **24**, 4575 (1991).
- [57] P. Ribeiro, J. Vidal, and R. Mosseri, *Phys. Rev. E* **78**, 021106 (2008).
- [58] R. Barnett, A. Turner, and E. Demler, *Phys. Rev. Lett.* **97**, 180412 (2006).
- [59] R. Barnett, A. Turner, and E. Demler, *Phys. Rev. A* **76**, 013605 (2007).
- [60] R. Barnett, S. Mukerjee, and J. E. Moore, *Phys. Rev. Lett.* **100**, 240405 (2008).
- [61] H. Mäkelä and K.-A. Suominen, *Phys. Rev. Lett.* **99**, 190408 (2007).
- [62] P. Kolenderski and R. Demkowicz-Dobrzanski, *Phys. Rev. A* **78**, 052333 (2008).
- [63] P. Kolenderski, *Open Systems & Information Dynamics* **17(2)**, 107 (2009).
- [64] S. Tamaryan, T.-C. Wei, and D. Park, *Phys. Rev. A* **80**, 052315 (2009).
- [65] L. Chen, A. Xu, and H. Zhu, *Phys. Rev. A* **82**, 032301 (2010).
- [66] L. L. Whyte, *Am. Math. Mon.* **59**, 606 (1952).
- [67] P. M. L. Tammes, *Recueil des trav. bot. néerlandais* **27**, 1 (1930).
- [68] E. Weisstein, *MathWorld* ‘Spherical Code’, <http://mathworld.wolfram.com/SphericalCode.html>
- [69] J. J. Thomson, *Phil. Mag.* **7**, 237 (1904).
- [70] P. Leiderer, *Z. Phys. B* **98**, 303 (1995).
- [71] E. J. Davis, *Aerosol Sci. Technol.* **26**, 212 (1997).
- [72] C. J. Marzec and L. A. Day, *Biophys. J.* **65**, 2559 (1993).
- [73] A. D. Dinsmore *et al.*, *Science* **298**, 1006 (2002).
- [74] H. W. Kroto, J. R. Heath, S. C. O’Brien, R. F. Curl, and R. E. Smalley, *Nature* **318**, 162 (1985).
- [75] M. J. W. Dodgson and M. A. Moore, *Phys. Rev. B* **55**, 3816 (1997).
- [76] T. Erber and G. M. Hockney, *J. Phys. A: Math. Gen.* **24**, L1369 (1991).
- [77] J. Leech, *Math. Gazette* **41**, 81 (1957).
- [78] N. Ashby and W. E. Brittin, *Am. J. Phys.* **54**, 776 (1986).
- [79] E. L. Altschuler, T. J. Williams, E. R. Ratner, F. Dowla, and F. Wooten, *Phys. Rev. Lett.* **72**, 2671 (1994).
- [80] N. J. A. Sloane *et al.*, ‘Spherical Codes’, <http://www2.research.att.com/~njas/packings/>
- [81] D. J. Wales and S. Ulker, ‘Global Minima for the Thomson Problem’, online at <http://www-wales.ch.cam.ac.uk/~wales/CCD/Thomson/table.html>
- [82] A. A. Berezin, *Am. J. Phys.* **53**, 1036 (1985).
- [83] C. S. Ogilvy and L. Moser, *Am. Math. Mon.* **58**, 492 (1951).
- [84] a_0 can be set positive by means of the global phase, and for symmetric states with $|0\rangle$ as a CPP it is easy to verify that $a_1 = 0$ is a necessary condition for the partial derivatives of $|\langle\psi|\omega\rangle|^{\otimes n}$ being zero at $|\omega\rangle = |0\rangle$.
- [85] The ceiling function $\lceil x \rceil$ is the smallest integer not less than x .
- [86] E. Marx, *J. Franklin Inst.* **290**, 71 (1970).
- [87] K. Schütte and B. L. Van der Waerden, *Math. Ann.* **123**, 96 (1951).
- [88] J. Martin, O. Giraud, P. A. Braun, D. Braun, and T. Bastin, *Phys. Rev. A* **81**, 062347 (2010).
- [89] M. Abramowitz and I. A. Stegun, *Pocketbook of Mathematical Functions* (Verlag Harri Deutsch, Frankfurt, 1984).